

Probabilistic Models with Deep Neural Networks

Andrés R. Masegosa^{a,*}, Rafael Cabañas^b, Helge Langseth^c, Thomas D. Nielsen^d,
Antonio Salmerón^a

^a*Department of Mathematics, University of Almería, 04120 Almería, Spain*

^b*Istituto Dalle Molle di Studi sull'Intelligenza Artificiale (IDSIA), CH-6928 Manno (Lugano), Switzerland*

^c*Norwegian University of Science and Technology, NO-7491 Trondheim, Norway*

^d*Aalborg University, DK-9220 Aalborg, Denmark*

Abstract

Recent advances in statistical inference have significantly expanded the toolbox of probabilistic modeling. Historically, probabilistic modeling has been constrained to (i) very restricted model classes where exact or approximate probabilistic inference were feasible, and (ii) small or medium-sized data sets which fit within the main memory of the computer. However, developments in variational inference, a general form of approximate probabilistic inference originated in statistical physics, are allowing probabilistic modeling to overcome these restrictions: (i) Approximate probabilistic inference is now possible over a broad class of probabilistic models containing a large number of parameters, and (ii) scalable inference methods based on stochastic gradient descent and distributed computation engines allow to apply probabilistic modeling over massive data sets. One important practical consequence of these advances is the possibility to include deep neural networks within a probabilistic model to capture complex non-linear stochastic relationships between random variables. These advances in conjunction with the release of novel probabilistic modeling toolboxes have greatly expanded the scope of application of probabilistic models, and allow these models to take advantage of the recent strides made by the deep learning community. In this paper we review the main concepts, methods and tools needed to use deep neural networks within a probabilistic modeling framework.

^{*}Corresponding author

Email addresses: andresmasegosa@ual.es (Andrés R. Masegosa), rcaban@idsia.ch (Rafael Cabañas), helge.langseth@ntnu.no (Helge Langseth), tdn@cs.aau.dk (Thomas D. Nielsen), antonio.salmeron@ual.es (Antonio Salmerón)

Keywords: Deep probabilistic modeling, Variational inference, Neural networks, Latent variable models, Bayesian learning

1. Introduction

The seminal works of Pearl (1988) and Lauritzen (1992) about probabilistic graphical models (PGMs) made probabilistic modeling an indispensable tool for dealing with uncertainty within many different fields, such as artificial intelligence (Russell and Norvig, 2016), statistics (Hastie et al., 2001), and machine learning (Bishop, 2006; Murphy, 2012). PGMs have been present in the literature for over 30 years and have become a well established and highly influential body of research. At the same time, the problem of computing the posterior probability over hidden quantities given the known evidence, also known as the inference problem (Pearl, 1988; Lauritzen, 1992; Jensen and Nielsen, 2007; Koller and Friedman, 2009), has been the corner-stone, as well as the bottleneck, of the feasibility and applicability of probabilistic modeling.

In the beginning, the first proposed inference algorithms (Pearl, 1988; Lauritzen, 1992) were able to compute this posterior in an exact way by exploiting the conditional independence relationships encoded by the graphical structure of the model. However, the set of supported probability distributions was strongly restricted, and mainly multinomial and conditional linear Gaussian distributions were used (Jensen and Nielsen, 2007; Koller and Friedman, 2009). Researchers quickly realized that the high computational costs of these exact inference schemes made them inappropriate for dealing with the complex stochastic dependency structures that arise in many relevant problems (Koller and Friedman, 2009) and, consequently, approximate inference methods became a main research focus.

Markov Chain Monte Carlo methods were one of the first approximate methods employed to make inference over complex PGMs (Gilks et al., 1995; Salmerón et al., 2000; Plummer, 2003). These techniques are extremely versatile and powerful, and they are able to approximate complex posterior distributions. However, they have serious issues like problems of convergence of the underlying Markov chain and poor mixing when approximating high dimensional distributions (Gilks et al., 1995). Com-

puting such high dimensional posteriors started to become relevant in many domains, specifically when researchers applied a Bayesian approach to learn the parameters of their PGMs from data (Bishop, 2006; Murphy, 2012; Blei, 2014). In this case, the model parameters are treated as unobserved random variables, and the learning problem reduces to computing the posterior probability over the parameters. For models with a large number of parameters, the approach leads to high dimensional posteriors where the application of Monte Carlo methods becomes infeasible. These issues gave rise to the development of alternative approximate inference schemes.

Belief propagation (BP) (Pearl, 1988; Murphy et al., 1999), and the closely related Expectation propagation (EP) (Minka, 2001), have been successfully used to overcome many of the limitations of Monte Carlo methods. They are deterministic techniques for approximate inference, which can be implemented using a message-passing scheme that takes advantage of the graph structure of the PGM and, hence, the underlying conditional independence relationships among variables. In terms of distributional assumptions, BP has mainly been used on multinomial and Gaussian distributions. Although EP allows for a more general family of distributions, it is restricted by the need to define a non-trivial quotient operation between the involved densities. While these techniques overcame some of the difficulties of Monte Carlo methods, they presented two new issues: (i) they do not guarantee the convergence to an approximate and meaningful solution; and (ii) do not scale to the kind of models that appear in the context of Bayesian learning (Murphy, 2012; Blei, 2014). Again, these challenges motivated researchers to look into alternative approximate inference schemes.

Variational methods (Wainwright and Jordan, 2008) were firstly explored in the context of PGMs during the late 90s (Jordan et al., 1999), inspired by their successful application in inference problems encountered in statistical physics. Like BP and EP, they are deterministic approximate inference techniques. The main innovation is to cast the inference problem as a minimization-problem with a well defined loss function, namely the negative Evidence Lower BOund (ELBO) function, which acts as an inference proxy. In general, variational methods guarantee convergence to a local maximum of this ELBO function, and therefore to a meaningful solution. By transforming the inference problem into a continuous optimization problem, variational methods

can take advantage of recent advances in continuous optimization theory. This was the case for the widely adopted stochastic gradient descent algorithm (Bottou, 2010), which was successfully used by the machine learning community to scale learning algorithms to big data sets. This same learning algorithm was adapted to variational inference by Hoffman et al. (2013), giving the opportunity to apply probabilistic modeling to problems involving massive data sets. In terms of distributional assumptions, these variational inference methods were restricted to the conjugate exponential family (Barndorff-Nielsen, 2014), where the gradient of the ELBO wrt. model parameters can be computed in closed-form (Winn and Bishop, 2005). Ad-hoc approaches were developed for models outside this distributional family.

From the start of the field at end of the 1980’s and up to around 2010, probabilistic models had mainly been focused on using distributions from the conjugate exponential family, even though this family of distributions is only able to model linear relationships between the random variables (Winn and Bishop, 2005). On the other hand, one of the reasons for the success of deep learning methods (Goodfellow et al., 2016) is the ability of deep neural networks to model non-linear relationships among high-dimensional objects, as is observed, e.g., between the pixels of an image or the words of a document. Recent advances in variational inference (Kingma and Welling, 2013; Ranganath et al., 2014) gave the opportunity to integrate deep neural networks into probabilistic models to capture such non-linear relationships among random variables. This gave rise to a whole new family of probabilistic models, which are often denoted *deep generative models* (Hinton, 2009, 2012; Goodfellow et al., 2014; Salakhutdinov, 2015). This new family of probabilistic models are able to encode objects like images, text, audio, and video probabilistically, thus bringing many of the recent advances produced by the deep learning community to the field of probabilistic modeling. The release of modern probabilistic programming languages (Tran et al., 2016, 2018; Bingham et al., 2018; Cabañas et al., 2019) relying on well established deep learning learning engines like Tensorflow (Abadi et al., 2015), PyTorch (Paszke et al., 2017).

In this paper we give a coherent overview of the key concepts and methods needed to introduce deep neural networks into probabilistic modeling. The present paper differs from other recent reviews of, e.g., deep generative models (Salakhutdinov, 2015)

and variational inference methods (Zhang et al., 2018), as we also go into details regarding implementation of such models using relevant software tools. To this end, the paper is accompanied by online material, where the running examples of the paper are coded to illustrate the theoretical concepts and methods¹.

2. Probabilistic Models within the Conjugate Exponential Family

2.1. Latent Variable Models

The conjugate exponential family of distributions (Barndorff-Nielsen, 2014) covers a broad and widely used range of probability distributions and density functions such as Multinomial, Normal, Gamma, Dirichlet and Beta. They have been used by the machine learning community (Bishop, 2006; Koller and Friedman, 2009; Murphy, 2012) due to their convenient properties related to parameter learning and inference tasks.

In the following we focus on probabilistic graphical models with structure as shown in Figure 1, and where the full model belongs to the conjugate exponential family. These models are also known as latent variable models (LVMs) (Bishop, 1998; Blei, 2014). LVMs are widely used as a tool for discovering patterns in data sets. The model in Figure 1 captures “local” patterns, which are specific to sample i of the data, using unobservable (or latent) random variables denoted by Z_i . “Global” patterns, those that are shared among all the samples of the data set, are modelled by means of a set of latent random variables denoted by β . The observed data sample i , X_i , is modelled as random variables whose distribution is conditioned on both the local (Z_i) and global (β) latent variables. α , a vector of fixed hyper-parameters, is also included in the model.

While the model structure in Figure 1 at first sight can appear restrictive, it is in fact quite versatile, and many books contain entire sections devoted to LVMs (Bishop, 2006; Koller and Friedman, 2009; Murphy, 2012). For instance, LVMs include popular models like Latent Dirichlet Allocation (LDA) models used to uncover the hidden topics in a text corpora (Blei et al., 2003), mixture of Gaussian models to discover

¹<https://github.com/PGM-Lab/ProbModelingDNNs>

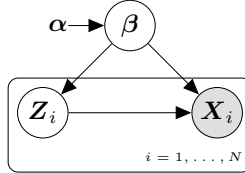


Figure 1: Structure of the probabilistic model examined in this paper, defined for a sample of size N .

hidden clusters in data (Bishop, 2006), probabilistic principal component analysis for dimensionality reduction (Tipping and Bishop, 1999), and models to capture drift in a data stream (Masegosa et al., 2017a). They have been used for knowledge extraction from GPS data (Kucukelbir et al., 2017), genetic data (Pritchard et al., 2000), graph data (Kipf and Welling, 2016), and so on.

The joint distribution of this probabilistic model factorizes into a product of local terms and a global term as

$$p(\mathbf{x}, \mathbf{z}, \boldsymbol{\beta}) = p(\boldsymbol{\beta}) \prod_{i=1}^N p(\mathbf{x}_i, \mathbf{z}_i | \boldsymbol{\beta}),$$

where N is the number of samples. As can be seen, the local latent variables \mathbf{Z}_i are assumed conditionally independent given the global latent variables $\boldsymbol{\beta}$.

Another standard assumption in these models is known as the assumption of *complete conditional form* (Hoffman et al., 2013). Now, the distribution of one latent variable given the other variables in the model can be expressed in exponential family form,

$$\begin{aligned} \ln p(\boldsymbol{\beta} | \mathbf{x}, \mathbf{z}) &= h_g(\boldsymbol{\beta}) + \boldsymbol{\eta}_g(\mathbf{x}, \mathbf{z})^\top \mathbf{t}(\boldsymbol{\beta}) - a_g(\boldsymbol{\eta}_g(\mathbf{x}, \mathbf{z})), \\ \ln p(\mathbf{z}_i | \mathbf{x}_i, \boldsymbol{\beta}) &= h_l(\mathbf{z}_i) + \boldsymbol{\eta}_l(\mathbf{x}_i, \boldsymbol{\beta})^\top \mathbf{t}(\mathbf{z}_i) - a_l(\boldsymbol{\eta}_l(\mathbf{x}_i, \boldsymbol{\beta})). \end{aligned} \quad (1)$$

where the scalar functions $h(\cdot)$ and $a(\cdot)$ are the base measures and the log-normalizers functions, respectively; the vector functions $\boldsymbol{\eta}(\cdot)$ and $\mathbf{t}(\cdot)$ are the *natural parameter* and the *sufficient statistics* vectors, respectively. The subscripts of these functions, here g for “global” and l for “local”, are used to signify that the different functions differ between variables. The subscripts will be removed when clear from context.

By conjugacy properties, the above assumptions also ensure that the conditional

distribution $p(\mathbf{x}_i, \mathbf{z}_i | \boldsymbol{\beta})$ is in the exponential family,

$$\ln p(\mathbf{x}_i, \mathbf{z}_i | \boldsymbol{\beta}) = \ln h(\mathbf{x}_i, \mathbf{z}_i) + \boldsymbol{\beta}^T \mathbf{t}(\mathbf{x}_i, \mathbf{z}_i) - a(\boldsymbol{\beta}), \quad (2)$$

and, similarly, for the prior distribution $p(\boldsymbol{\beta})$,

$$\ln p(\boldsymbol{\beta}) = \ln h_{\boldsymbol{\beta}}(\boldsymbol{\beta}) + \boldsymbol{\alpha}^T \mathbf{t}_{\boldsymbol{\beta}}(\boldsymbol{\beta}) - a_{\boldsymbol{\beta}}(\boldsymbol{\alpha}). \quad (3)$$

Combining Equation (2) and Equation (3), we see that the posterior $p(\boldsymbol{\beta} | \mathbf{x}, \mathbf{z})$ remains in the same distribution family as the prior $p(\boldsymbol{\beta})$ (that is, we have conjugacy) and, in consequence, the natural parameter of the global posterior $\boldsymbol{\eta}_g(\mathbf{x}, \mathbf{z})$ can be expressed as

$$\boldsymbol{\eta}_g(\mathbf{x}, \mathbf{z}) = \boldsymbol{\alpha} + \sum_{i=1}^N \mathbf{t}(\mathbf{x}_i, \mathbf{z}_i).$$

This representation of the *complete conditional* will be used later to derive the variational inference scheme over this model.

Example 1 Principal Component Analysis (PCA) is a classic statistical technique for dimensionality reduction. It defines a mapping between the d -dimensional data-representation of a point \mathbf{x} and its k -dimensional latent representation, \mathbf{z} . The latent representation is known as the *scores*, and the affine transformation is performed using the *loading matrix* $\boldsymbol{\beta}$, which has dimensions $k \times d$.

Algorithm 1 Pseudo-code of the generative model of a probabilistic PCA model.

```

# Sample from global random variables
 $\beta_{u,v} \sim \mathcal{N}(0, 1)$  # Sample for  $u = 1, \dots, k, v = 1, \dots, d$ .
for  $i = 1, \dots, N$  do
    # Sample from the local latent variables
     $\mathbf{z}_i \sim \mathcal{N}(\mathbf{0}, \mathbf{I})$ 
    # Sample from the observed variables
     $\mathbf{x}_i \sim \mathcal{N}(\boldsymbol{\beta}^T \mathbf{z}_i, \sigma_{\mathbf{x}}^2 \mathbf{I})$ 
end for

```

A simplified probabilistic view of PCA (Tipping and Bishop, 1999) is given in Algorithm 1, which provides pseudo-code for the generative process of a probabilistic PCA model. This model is obviously an LVM, as the loadings represented by β are global latent variables and Z_i is the vector of local latent variables associated with the i -th element in the sample.

This model belongs to this conjugate exponential family with complete conditionals, because the joint of $p(x, z, \beta)$ is multivariate Normal and, by standard properties of the multivariate Normal distribution, the conditional $p(\beta|z, x)$ and $p(z_i|x_i, \beta)$ are both conditional multivariate Gaussians. A multivariate Normal distribution with mean μ and covariance matrix Σ is a member of the exponential family with natural parameters $\eta = [\Sigma^{-1}\mu, -1/2\Sigma^{-1}]^T$ and sufficient statistics $t(x) = [x, xx^T]^T$.

Note that while this linear relationship between the latent and the observed variables is a strong limitation of this model (Schölkopf et al., 1998), it guarantees that the model belongs to conjugate exponential family. Using a non-linear relationship would put PCA outside this model family and would prevent, as we will see in the next section, the use of efficient inference algorithms to calculate $p(\beta|z, x)$ and $p(z_i|x_i, \beta)$. Similarly, if the variance parameter σ_x (see Algorithm 1) depend on the latent variables z_i , the model falls outside the conjugate exponential family.

Figure 2.1 illustrates the behavior of Probabilistic PCA as a feature reduction method on two different data sets, *Iris* and (a reduced version of) *MNIST*. The data is projected from data-dimension $d = 4$ (Iris) or $d = 784$ (MNIST) down into $k = 2$ latent dimensions. As can be seen, the method captures some of the underlying structure in the Iris-data, and even generates a representation where the three classes of the flower can be separated. On the other hand, the MNIST representation appears less informative. Images of the three digits “1”, “2” and “3” are given to the PCA, but even though these three groups of images are quite distinct, the learned representation is not able to clearly separate the classes from one another. As we

will see later in this paper, when we consider a more expressive mappings between the local latent \mathbf{Z}_i and \mathbf{X}_i (using artificial neural networks), the latent representations will become more informative.

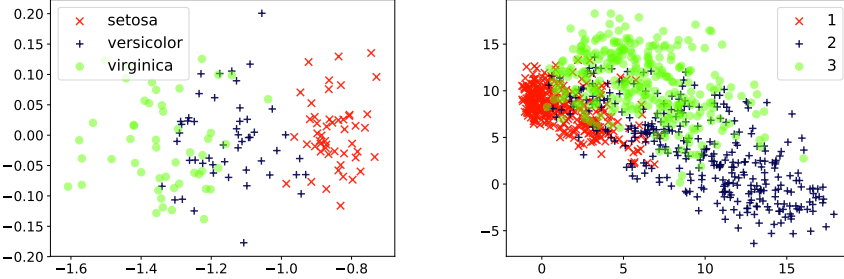


Figure 2: 2-dimensional latent representations resulting of applying a probabilistic PCA of: **(Left)** the iris dataset (Fisher, 1936) and **(Right)** a subset of 1000 instances from the MNIST dataset (LeCun et al., 1998) corresponding to the handwritten digits 1, 2 and 3.

2.2. Mean-Field Variational Inference

The problem of Bayesian inference reduces to computing the posterior over the unknown quantities (i.e. the global and local latent variables β and z , respectively) given the observations,

$$p(\beta, z | \mathbf{x}) = \frac{p(\mathbf{x} | z, \beta) p(z | \beta) p(\beta)}{\int \int p(\mathbf{x} | z, \beta) p(z | \beta) p(\beta) dz d\beta}.$$

Computing the above posterior is intractable for many interesting models, because it requires to solve the complicated multidimensional integral in the denominator. As commented in the introduction, variational inference (VI) methods are one of the best performing options to address this problem. In this section we revise the main ideas behind this approach.

Example 2 Computing $p(\beta, z | \mathbf{x})$ for the probabilistic PCA model described in Example 1 is not feasible since the integral

$$p(\mathbf{x}) = \int \int p(\mathbf{x} | z, \beta) p(z | \beta) p(\beta) dz d\beta$$

is intractable. The source of the problem is that $p(\mathbf{x}|\boldsymbol{\beta}) = \int p(\mathbf{x}|\mathbf{z}, \boldsymbol{\beta})p(\mathbf{z}|\boldsymbol{\beta})d\mathbf{z}$ is not in the conjugate exponential family.

Variational inference is a deterministic technique that finds a tractable approximation to an intractable (posterior) distribution. We will use q to denote the approximation, and use p to signify the true distribution (like $p(\boldsymbol{\beta}, \mathbf{z}|\mathbf{x})$ in the example above). More specifically, let \mathcal{Q} denote a set of possible approximations q . Now, VI solves the following optimization problem:

$$\min_{q \in \mathcal{Q}} KL(q||p), \quad (4)$$

where KL denotes the Kullback-Leibler divergence between two probability distributions. For the specific problem at hand, this general formulation is more precisely written as

$$\min_{q(\boldsymbol{\beta}, \mathbf{z}) \in \mathcal{Q}} KL(q(\boldsymbol{\beta}, \mathbf{z})||p(\boldsymbol{\beta}, \mathbf{z}|\mathbf{x}))$$

Notice that while q depends on the observations \mathbf{x} , it is customary to make this implicit in the notation, and write, e.g., $q(\boldsymbol{\beta}, \mathbf{z})$ instead of $q(\boldsymbol{\beta}, \mathbf{z}|\mathbf{x})$. In practice, one will typically posit that \mathcal{Q} is a convenient distributional family indexed by some parameters, say $\boldsymbol{\theta}$, and the minimization of Equation (4) amounts to finding the parameters $\boldsymbol{\theta}^*$ that minimize the KL divergence.

Under the *mean field* variational approach, the approximation family \mathcal{Q} is assumed to fully factorize. Following the notation of Hoffman et al. (2013), we have that

$$q(\boldsymbol{\beta}, \mathbf{z}|\boldsymbol{\lambda}, \boldsymbol{\phi}) = q(\boldsymbol{\beta}|\boldsymbol{\lambda}) \prod_{i=1}^N q(\mathbf{z}_i|\boldsymbol{\phi}_i), \quad (5)$$

where $\boldsymbol{\lambda}$ parameterizes the variational distribution of $\boldsymbol{\beta}$, while $\boldsymbol{\phi}_i$ has the same role for the variational distribution of \mathbf{z}_i .

Furthermore, if the model is model in the conjugate exponential family, each factor in the variational distribution is assumed to belong to the same family of the model's *complete conditionals* (see Equation (1)),

$$\begin{aligned} \ln q(\boldsymbol{\beta}|\boldsymbol{\lambda}) &= h(\boldsymbol{\beta}) + \boldsymbol{\lambda}^T \mathbf{t}(\boldsymbol{\beta}) - a(\boldsymbol{\lambda}), \\ \ln q(\mathbf{z}_i|\boldsymbol{\phi}_i) &= h(\mathbf{z}_i) + \boldsymbol{\phi}_i^T \mathbf{t}(\mathbf{z}_i) - a(\boldsymbol{\phi}_i). \end{aligned} \quad (6)$$

To solve the minimization problem in Equation (4), the variational approach exploits the transformation

$$\ln p(\mathbf{x}) = \mathcal{L}(\boldsymbol{\lambda}, \boldsymbol{\phi}) + KL(q(\boldsymbol{\beta}, \mathbf{z}|\boldsymbol{\lambda}, \boldsymbol{\phi})||p(\boldsymbol{\beta}, \mathbf{z}|\mathbf{x})), \quad (7)$$

where \mathcal{L} can be expressed as

$$\mathcal{L}(\boldsymbol{\lambda}, \boldsymbol{\phi}) = \mathbb{E}_q[\ln p(\mathbf{x}, \mathbf{z}, \boldsymbol{\beta})] - \mathbb{E}_q[\ln q(\boldsymbol{\beta}, \mathbf{z}|\boldsymbol{\lambda}, \boldsymbol{\phi})]. \quad (8)$$

\mathcal{L} is of interest in its own right. Notice in particular that \mathcal{L} in Equation (7) is a *lower bound* of $\ln p(\mathbf{x})$ since the KL-divergence is non-negative. For this reason, \mathcal{L} is usually referred to as the ELBO (Evidence Lower BOund). Furthermore, as $\ln p(\mathbf{x})$ is constant in the optimization wrt. q , minimizing the KL divergence in Equation (4) is equivalent to maximizing the lower bound \mathcal{L} . Variational methods maximize \mathcal{L} using gradient based techniques.

The key advantage of having a conjugate exponential model is that the gradients of \mathcal{L} wrt. its parameters can always be computed in closed form (Winn and Bishop, 2005). This is important, as it leads to a natural scheme in which the parameters are updated iteratively: For a parameter θ_j , simply choose the value θ_j^* so that $\nabla_{\theta_j} \mathcal{L}(\boldsymbol{\theta})|_{\boldsymbol{\theta}:\theta_j=\theta_j^*} = 0$. In practice it is beneficial to use the *natural gradients*, which is the standard gradient pre-multiplied by the inverse of the Fisher information matrix, to account for the Riemannian geometry of the parameter space (Amari, 1998).

The gradients with respect to the variational parameters $\boldsymbol{\lambda}$ and $\boldsymbol{\phi}$ can be computed as follows,

$$\begin{aligned} \nabla_{\boldsymbol{\lambda}}^{nat} \mathcal{L}(\boldsymbol{\lambda}, \boldsymbol{\phi}) &= \boldsymbol{\alpha} + \sum_{i=1}^N \mathbb{E}_{\phi_i}[\mathbf{t}(\mathbf{x}_i, \mathbf{z}_i)] - \boldsymbol{\lambda}, \\ \nabla_{\phi_i}^{nat} \mathcal{L}(\boldsymbol{\lambda}, \boldsymbol{\phi}) &= \mathbb{E}_{\lambda}[\boldsymbol{\eta}_l(\mathbf{x}_i, \boldsymbol{\beta})] - \boldsymbol{\phi}_i, \end{aligned} \quad (9)$$

where ∇^{nat} denotes natural gradients and $\mathbb{E}_{\phi_i}[\cdot]$ and $\mathbb{E}_{\lambda}[\cdot]$ denote expectations with respect to $q(\mathbf{z}_i|\boldsymbol{\phi}_i)$ and $q(\boldsymbol{\beta}|\boldsymbol{\lambda})$, respectively.

From the above gradients we can derive a coordinate ascent algorithm to optimize

the ELBO function with the following coordinate ascent rules,

$$\begin{aligned}\boldsymbol{\lambda}^* &= \arg \max_{\boldsymbol{\lambda}} \mathcal{L}(\boldsymbol{\lambda}, \boldsymbol{\phi}) = \boldsymbol{\alpha} + \sum_{i=1}^N \mathbb{E}_{\phi_i} [\mathbf{t}(\mathbf{x}_i, \mathbf{z}_i)], \\ \boldsymbol{\phi}_i^* &= \arg \max_{\phi_i} \mathcal{L}(\boldsymbol{\lambda}, \boldsymbol{\phi}) = \mathbb{E}_{\lambda} [\boldsymbol{\eta}_l(\mathbf{x}_i, \boldsymbol{\beta})].\end{aligned}\quad (10)$$

By iteratively running the above updating equations, we are guaranteed to (i) monotonically increase the ELBO function at every time step and (ii) to converge to a stationary point of the ELBO function or, equivalently, the function minimizing Equation (4).

Example 3 For the PCA model in Example 1, the variational distributions are

$$\begin{aligned}q(\boldsymbol{\beta} | \boldsymbol{\mu}_{\beta}, \boldsymbol{\Sigma}_{\beta}) &= \mathcal{N}(\boldsymbol{\beta} | \boldsymbol{\mu}_{\beta}, \boldsymbol{\Sigma}_{\beta}), \\ q(\mathbf{z}_i | \boldsymbol{\mu}_{z_i}, \boldsymbol{\Sigma}_{z_i}) &= \mathcal{N}(\mathbf{z}_i | \boldsymbol{\mu}_{z_i}, \boldsymbol{\Sigma}_{z_i}).\end{aligned}$$

Given the above variational family, the coordinate updating equations derived from Equation (10) can be written, after some algebraic manipulations, as (Bishop, 2006)

$$\begin{aligned}\boldsymbol{\Sigma}_{\beta} &= \left(\sum_{i=1}^N \mathbb{E}[\mathbf{z}_i \mathbf{z}_i^T] + \sigma_x^2 \mathbf{A} \right)^{-1}, \\ \boldsymbol{\mu}_{\beta} &= \left[\sum_{i=1}^N \mathbf{x}_i \mathbb{E}[\mathbf{z}_i] \right]^T \boldsymbol{\Sigma}_{\beta}, \\ \boldsymbol{\Sigma}_{z_i} &= (\mathbf{I} + \boldsymbol{\mu}_{\beta}^T \boldsymbol{\mu}_{\beta} / \sigma_x^2)^{-1}, \\ \boldsymbol{\mu}_{z_i} &= \boldsymbol{\Sigma}_{z_i} \boldsymbol{\mu}_{\beta}^T \mathbf{x}_i / \sigma_x^2,\end{aligned}$$

where \mathbf{A} is a diagonal matrix with element at index i given by $d / \boldsymbol{\mu}_{\beta, i}^T \boldsymbol{\mu}_{\beta, i}$.

Again, we have a set of closed-form equations which guarantees convergence to the solution of the inference problem. We should note that this is possible due to the strong assumptions imposed both on the probabilistic model p and on the family of variational approximations \mathcal{Q} .

2.3. Scalable Variational Inference

Performing VI on large data sets (measured by the number of samples, N) raises many challenges. Firstly, the model itself may not fit in memory, and, secondly, the cost

of computing the gradient of the ELBO with respect to λ linearly depends on the size of the data set (see Equation (9)), which can be prohibitively expensive when N is very large. Stochastic Variational inference (SVI) (Hoffman et al., 2013) is a popular method for scaling VI to massive data sets, and relies on stochastic optimization techniques (Robbins and Monro, 1951; Bottou, 2010).

We start by re-parameterizing the ELBO so that \mathcal{L} is expressed only in terms of the global parameters λ . This is done by defining

$$\mathcal{L}(\lambda) = \mathcal{L}(\lambda, \phi^*(\lambda)), \quad (11)$$

where $\phi^*(\lambda)$ is defined as in Equation (10), i.e. it returns a local optimum of the local variational parameters ϕ for a given λ . Now $\mathcal{L}(\lambda)$ has the following form:

$$\begin{aligned} \mathcal{L}(\lambda) &= \mathbb{E}_q[\ln p(\beta)] - \mathbb{E}_q[\ln q(\beta|\lambda)] \\ &+ \sum_{i=1}^N \max_{\phi_i} \{ \mathbb{E}_q[\ln p(\mathbf{x}_i, \mathbf{z}_i|\beta)] - \mathbb{E}_q[\ln q(\mathbf{z}_i|\phi_i)] \} \end{aligned} \quad (12)$$

As shown by Hoffman et al. (2013), we can compute the gradient of $\mathcal{L}(\lambda)$ by first finding $\phi^*(\lambda)$, and then compute the gradient w.r.t. λ while keeping $\phi^*(\lambda)$ fixed (because $\nabla_\lambda \mathcal{L}(\lambda) = \nabla_\lambda \mathcal{L}(\lambda, \phi^*(\lambda))$). By exploiting properties of the conjugate exponential family, the natural gradient with respect to λ can be computed in closed-form as

$$\nabla_\lambda^{nat} \mathcal{L}(\lambda) = \alpha + \sum_{i=1}^N \mathbb{E}_{\phi_i^*}[t(\mathbf{x}_i, \mathbf{z}_i)] - \lambda.$$

The key idea behind SVI is to compute unbiased albeit noisy estimates of $\nabla_\lambda^{nat} \mathcal{L}$, denoted $\hat{\nabla}_\lambda^{nat} \mathcal{L}$, by randomly selecting a mini-batch of M data samples, and then define

$$\hat{\nabla}_\lambda^{nat} \mathcal{L}(\lambda) = \alpha + \frac{N}{M} \sum_{m=1}^M \mathbb{E}_{\phi_i^*}[t(\mathbf{x}_{i_m}, \mathbf{z}_{i_m})] - \lambda,$$

where i_m is the variable index from the subsampled mini-batch. It is immediate that $\mathbb{E}[\hat{\nabla}_\lambda^{nat} \mathcal{L}] = \nabla_\lambda^{nat} \mathcal{L}$, hence the estimator is unbiased. Utilizing stochastic optimization theory (Robbins and Monro, 1951), the ELBO can be maximized by following noisy estimates of the gradient,

$$\lambda_{t+1} = \lambda_t + \rho_t \hat{\nabla}_\lambda^{nat} \mathcal{L}(\lambda_t), \quad (13)$$

if the learning rate ρ_t satisfies the Robbins-Monro conditions². In this case the above updating equation is guaranteed to converge to a stationary point of the ELBO.

To choose the size of the mini-batch M , two conflicting issues should be considered: Smaller values of M (i.e., $M \ll N$) leads to a reduction in the computational complexity of computing the gradient, while larger values of M (i.e., $M \gg 1$) reduces the variance of the estimator. The optimal value for M is problem dependent (Li et al., 2014).

Alternative ways to scale up variational inference in conjugate exponential models involve the use of distributed computing clusters. For example, Masegosa et al. (2017b) assume that the data set is stored in a distributed way among different machines. Then the problem of computing the ELBO's gradient given in Equation (9) is scaled up by distributing the computation of the gradient $\nabla_{\phi_i}^{nat} \mathcal{L}(\lambda, \phi)$ so that each machine computes this term for those samples that are locally stored. Finally, all the terms are sent to a master node which aggregates them and compute the gradient $\nabla_{\lambda}^{nat} \mathcal{L}(\lambda, \phi)$ (see Equation (9)).

Example 4 In Example 3 we detailed the variational updating equations for the Probabilistic PCA model introduced in Example 1. In order to update μ_{β}^* we need to iterate over the whole data set. Furthermore, the number of local variational parameters $\mu_{z_i}^*$ and $\Sigma_{z_i}^*$ is equal to the number of data points. Therefore, if N is very large, the computation of these variational updating equations becomes infeasible.

Following the methodology presented in this section, we can obtain a new set of variational updating equations,

$$\begin{aligned}\Sigma_{\beta,t+1} &= \left[(1 - \rho_t) \Sigma_{\beta,t}^{-1} + \rho_t \left(\frac{N}{M} \sum_{m=1}^M \mathbb{E}_{t,i_m} [\mathbf{Z}_{i_m} \mathbf{Z}_{i_m}^T] + \sigma_x^2 \mathbf{A} \right) \right]^{-1}, \\ \mu_{\beta,t+1} &= (1 - \rho_t) \mu_{\beta,t+1} + \rho_t \left(\frac{N}{M} \sum_{m=1}^M \mathbf{x}_{i_m} \mathbb{E}_{t,i_m} [\mathbf{Z}_{i_m}] \right)^T \Sigma_{\beta,t+1},\end{aligned}$$

where $\{i_1, \dots, i_M\}$ are the indexes of the mini-batch, and $\mathbb{E}_{t,i_m}[\cdot]$ denotes

²A sequence $\{\rho_t\}_{t=1}^{\infty}$ satisfies the Robbins-Monro conditions if $\sum_{t=1}^{\infty} \rho_t = \infty$ and $\sum_{t=1}^{\infty} \rho_t^2 < \infty$.

expectations when Z_{i_m} follows a Normal distribution with parameters

$$\begin{aligned}\boldsymbol{\Sigma}_{t,z_{i_m}} &= (\mathbf{I} + \sigma_x^{-2} \boldsymbol{\mu}_{\beta,t}^{\top} \boldsymbol{\mu}_{\beta,t})^{-1}, \\ \boldsymbol{\mu}_{t,z_{i_m}} &= \boldsymbol{\Sigma}_{t,z_{i_m}} \boldsymbol{\mu}_{\beta,t}^{\top} \mathbf{x}_{i_m} / \sigma_x^2;\end{aligned}$$

confer also Example 3. Using this set-up, we do not need to go thorough the full data set to get an update of the global variational parameters.

2.4. Variational Message Passing

So far we have treated the set of variables \mathbf{x} , \mathbf{z} and $\boldsymbol{\beta}$ as undividable blocks of variables without internal structure. However, as we are dealing with flexible probabilistic graphical models, these sets of variables can often encode conditional independencies that can be further exploited when using VI. *Variational message passing* (VMP) (Winn and Bishop, 2005) is a VI scheme which readily exploits such conditional independencies when performing approximate inference. Now, Z_i and X_i , the set of latent and observable variables associated to the i -th data sample, are separated into individual variables $Z_i = \{Z_{i,1}, \dots, Z_{i,K}\}$, and similarly for X_i . Additionally, $\boldsymbol{\beta}$ is regarded as a set of J separate random variables $\boldsymbol{\beta} = \{\beta_1, \dots, \beta_J\}$. Now, under the mean field assumption, the variational distribution is expressed as

$$q(\boldsymbol{\beta}, \mathbf{z} | \boldsymbol{\lambda}_i, \boldsymbol{\phi}) = \prod_{j=1}^J q(\beta_j | \boldsymbol{\lambda}_j) \prod_{i=1}^N \prod_{k=1}^K q(z_{i,k} | \boldsymbol{\phi}_{i,k}).$$

Using the VMP scheme, the gradients wrt. the variational parameters can be computed using a message-passing algorithm which exploits the conditional independencies between the variables in X_i , Z_i and $\boldsymbol{\beta}$. The flow of messages is similar to the one employed by loopy belief propagation (Pearl, 1988). The messages are expected sufficient statistics of the variables involved, and since the model is in the conjugate exponential family, both the messages and the update rules can be expressed analytically, leading to parameter updates akin to Equation (10); cf. Winn and Bishop (2005) for details.

3. Deep Neural Networks and Computational Graphs

3.1. Deep Neural Networks

An artificial neural network (ANN) (Hopfield, 1988) can be seen as a deterministic non-linear function $f(\cdot : \mathbf{W})$ parametrized by a matrix \mathbf{W} . An ANN with L hidden layers defines a mapping from a given input \mathbf{x} to a given output \mathbf{y} . This mapping is built by the recursive application of a sequence of (non-)linear transformations,

$$\begin{aligned} \mathbf{h}_0 &= \mathbf{r}_0(\mathbf{W}_0^T \mathbf{x}), \\ &\dots \\ \mathbf{h}_l &= \mathbf{r}_l(\mathbf{W}_{l-1}^T \mathbf{h}_{l-1}), \\ &\dots \\ \mathbf{y} &= \mathbf{r}_L(\mathbf{W}_L^T \mathbf{h}_L), \end{aligned} \tag{14}$$

where $\mathbf{r}_l(\cdot)$ defines the activation (non-linear) function at the l -th layer; standard activation functions include the *soft-max* function and the *relu* function (Goodfellow et al., 2016). \mathbf{W}_l are the parameters defining the linear transformation at the l -th layer, where the dimensionality of the target layer is defined by the size of \mathbf{W}_l . Deep neural networks (DNNs) is a renaming of classic ANNs, with the key difference that DNNs usually have a higher number of hidden layers compared to what classical ANNs used to have.

Learning a DNN from a given data set of input-output pairs (\mathbf{x}, \mathbf{y}) reduces to solving the optimization problem

$$\mathbf{W}^* = \arg \min_{\mathbf{W}} \sum_{i=1}^N \ell(y_i, f(\mathbf{x}_i; \mathbf{W})), \tag{15}$$

where $\ell(y_i, \hat{y}_i)$ is a loss function which defines the quality of the model, i.e, how well the output $\hat{y}_i = f(\mathbf{x}_i; \mathbf{W})$ returned by the DNN model matches the real output y_i . This continuous optimization problem is usually solved by applying a variant of the stochastic gradient descent method, which involves the computation of the gradient of the loss function with respect to the parameters of the ANN, $\nabla_{\mathbf{W}} \ell(y_i, f(\mathbf{x}_i; \mathbf{W}))$. The algorithm for computing this gradient in an ANN is known as the *back-propagation*

algorithm, which is based on the recursive application of the chain-rule of derivatives and typically implemented based in the computational graph of the ANN. Goodfellow et al. (2016) provides a detailed and modern introduction to this field.

3.2. Computational Graphs

Computational graphs have been extremely useful when developing algorithms and software packages for neural networks and other models in machine learning (Chen et al., 2015; Abadi et al., 2015; Paszke et al., 2017). The main idea of a computational graph is to express a (deterministic) function, as is the case of a neural network, as an acyclic directed graph defining a sequence of computational operations. A computational graph is composed of input and output nodes as well as operation nodes. The data and the parameters of the model serve as input nodes, whereas the operation nodes (represented as squares in the subsequent diagrams) correspond to the primitive operations of the network and also define the output of the network. The directed edges in the graph specify the inputs of each node. Input nodes are usually defined over tensors (n -dimensional arrays) and operations are thus similarly defined over tensors, thereby also enabling the computational graph to, e.g., process batches of data. Figure 3 shows a simple example of a computational graph.

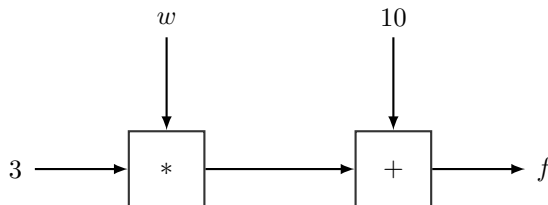


Figure 3: Example of a simple Computational Graph. Squared nodes denote operations, and the rest are input nodes. This computational graph encodes the operation $f = 3 \cdot w + 10$, where w is a variable wrt. which we can differentiate.

With computational graphs simple/primitive functions can be combined to form complex operations, and the vast majority of current neural networks can be defined using computational graphs. But the key strength of computational graphs is that they allow for automatic differentiation (Griewank, 1989). As shown in the previous section

(see Equation (15)), most neural network learning algorithms translate to a continuous optimization problem of a differentiable loss function often solved by a gradient descent algorithm. Automatic differentiation is a technique for automatically computing all the partial derivatives of the function encoded by a computational graph: once the graph has been defined using underlying primitive operations, derivatives are automatically calculated based on the “local” derivatives of these operations and the recursive application of the chain rule of derivatives, incurring only a small computational overhead. Before the use of computational graphs in deep learning, these derivatives had to be computed manually, giving rise to a slow and error-prone development process.

Example 5 Figure 4 provides an example of a computational graph encoding a neural network with x as input, \hat{y} as output, and two hidden layers. This computational graph also encodes the loss function $\ell(y, \hat{y})$.

As computational graphs can be defined over tensors, the above computational graph can encode the forward (and backward) pass of the neural network for a whole data batch x , and thereby also provide the loss (and the gradient) for this set of data samples. Algorithm 2 shows the pseudo-code description for defining and learning this neural network using standard gradient descent.

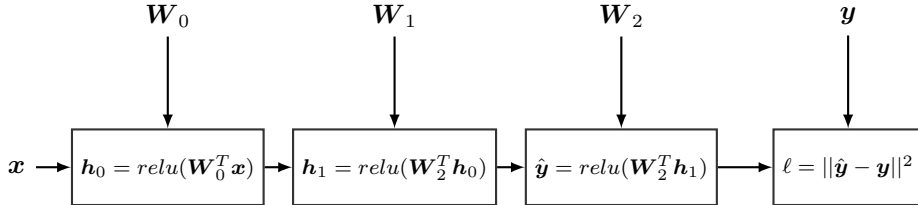


Figure 4: Example of a simple Computational Graph encoding a neural network with two hidden layers and the squared loss function. Note that each operation node encapsulates a part of the CG encoding the associated operations, we do not expand the whole CG for the sake of simplicity.

Algorithm 2 Pseudo-code of the definition and learning of a simple neural network.

input \mathbf{x}, \mathbf{y} the labels.

```
# Define the computational graph encoding the ANN and the loss function
 $\mathbf{W}_0, \mathbf{W}_1, \mathbf{W}_2 = \text{Parameters}()$ 
 $\mathbf{h}_0 = \text{relu}(\mathbf{W}_0^T \mathbf{x})$ 
 $\mathbf{h}_1 = \text{relu}(\mathbf{W}_1^T \mathbf{h}_0)$ 
 $\hat{\mathbf{y}} = \text{relu}(\mathbf{W}_2^T \mathbf{h}_1)$ 
 $\ell = \|\hat{\mathbf{y}} - \mathbf{y}\|^2$ 
# Follow the gradients until convergence.
 $\mathbf{W} = (\mathbf{W}_0, \mathbf{W}_1, \mathbf{W}_2)$ 
repeat
     $\mathbf{W} = \mathbf{W} - \rho \nabla_{\mathbf{W}} \ell$ 
until convergence
```

4. Probabilistic Models with Deep Neural networks

4.1. Deep Latent Variable Models

LVMs have usually been restricted to the conjugate exponential family because, in this case, inference is feasible (and scalable) as we showed in Section 2. But recent advances in VI (which will be reviewed in Section 5) have enabled LVMs to be extended with DNNs. Variational Auto-encoders (VAE) (Kingma and Welling, 2013; Doersch, 2016) are probably the most influential models combining LVMs and DNNs. VAEs extend the classical technique of principal component analysis (PCA) (Jolliffe, 2011) for data representation in lower-dimensional spaces. More precisely, Kingma and Welling (2013) extend the probabilistic version of the PCA model (Tipping and Bishop, 1999), where the relationship between the low-dimensional representation and the observed data is governed by a DNN, i.e. a highly non-linear function, as opposed to the standard linear transformation in the basic version of the PCA model. These models are able to capture more compact low-dimensional representations, especially in cases where data is high-dimensional but "lives" in a low-dimensional manifold (Pless and Souvenir, 2009). This is, e.g., the case for image data (Kingma and Welling,

2013; Kulkarni et al., 2015; Gregor et al., 2015; Sohn et al., 2015; Pu et al., 2016), text data (Semeniuta et al., 2017), audio data (Hsu et al., 2017), chemical molecules (Gómez-Bombarelli et al., 2018), to name some representative applications of this technique. We note that, in this section and in the following ones, we will use VAEs as a running example illustrating how DNNs can be used in probabilistic modeling.

VAEs have also given rise to a plethora of extensions of classic LVMs to their *deep counterpart*. For instance, Johnson et al. (2016) provides different examples of this approach and propose extensions of Gaussian mixture models, latent linear dynamical systems and latent switching linear dynamical systems with the non-linear relationships modelled by DNNs. Linderman et al. (2016) extend hidden semi-Markov models with recurrent neural networks. Zhou et al. (2015) and Card et al. (2017) propose extensions of popular LDA models (Blei et al., 2003) for uncovering topics in text data. Many other works are following the same trend (Chung et al., 2015; Jiang et al., 2016; Xie et al., 2016; Louizos et al., 2017).

Example 6 VAEs are widely adopted LVM containing DNNs (Kingma and Welling, 2013). Algorithm 3 provides a simplified pseudo-code description of the *generative part* of a VAE model. It can also be seen as a non-linear probabilistic PCA model, where the non-linearity is included in the form of an artificial neural network.

This model is quite similar to the PCA model presented in Example 1. The main difference comes from the conditional distribution of \mathbf{x} . In the PCA model, the mean of the normal distribution of \mathbf{x} linearly depends on \mathbf{z} through $\boldsymbol{\beta}$. In the VAE model, the mean depends on \mathbf{z} through a DNN parametrized by $\boldsymbol{\beta}$. This DNN is also known as the *decoder network* of the VAE (Kingma and Welling, 2013).

Note that some formulations of this model also include another DNN component, which connects \mathbf{z} with the variance σ^2 of the Normal distribution of \mathbf{x} ; for the sake of simplicity, we have not included this extension in the example.

Figure 5 experimentally illustrates the advantage of using a non-linear

PCA model over the classic PCA model. As can be seen, the non-linear version separates more clearly the three digits than the linear one.

We shall return to this example in Section 5.2, where we will introduce the so-called *encoder network* used for inference.

Algorithm 3 Pseudo-code of the generative model of a Variational Auto-encoder (or non-linear probabilistic PCA)

```

# Define the global parameters
 $\alpha_0, \beta_0, \alpha_1, \beta_1 \sim \mathcal{N}(\mathbf{0}, \mathbf{I})$ 
for  $i = 1, \dots, N$  do
    # Define the local latent variables
     $z_i \sim \mathcal{N}(\mathbf{0}, \mathbf{I})$ 
    # Define the ANN with a single hidden layer  $h_i$ 
     $h_i = \text{relu}(\beta_0^T z_i + \alpha_0)$ 
     $\mu_i = \beta_1^T h_i + \alpha_1$ 
    # Define the observed variables
     $x_i \sim \mathcal{N}(\mu_i, \sigma^2 \mathbf{I})$ 
end for

```

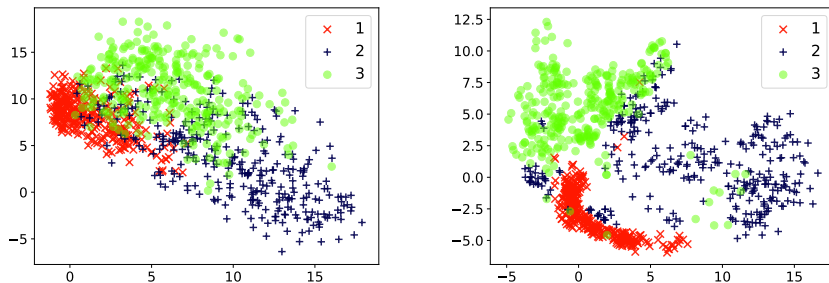


Figure 5: 2-dimensional latent representations of the the MNIST dataset resulting of applying: **(Left)** a standard probabilistic PCA (reproduced from Figure 2.1 to ease comparison), and **(Right)** a non-linear probabilistic PCA with a ANN containing a hidden layer of size 100 with a *relu* activation function.

LVMs with DNNs can also be found in the literature under the name of deep gen-

erative models (Hinton, 2009, 2012; Goodfellow et al., 2014; Salakhutdinov, 2015). These models highlight their capacity to generate data samples using probabilistic constructs that include DNNs. This new capacity has also provoked a strong impact within the deep learning community because it has opened up for the possibility of dealing with unsupervised learning problems, e.g., in the form of generative adversarial nets Goodfellow et al. (2014). This should be seen in contrast to the *classic deep learning methods*, which are mainly focused on supervised learning settings. In any case, this active area of research is out of the scope of this paper and contains many alternative models, which do not fall within the category of the models explored in this paper.

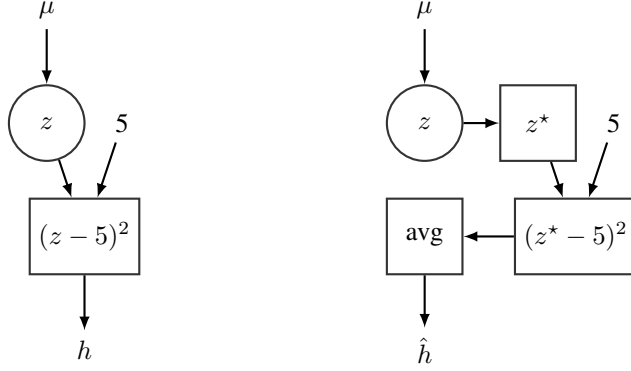
4.2. Stochastic Computational Graphs

One of the main reasons for the wide adoption of deep learning has been the availability of (open-source) software tools containing robust and well-tested implementations of the main building blocks for defining and learning DNNs (Abadi et al., 2015; Paszke et al., 2017). Recently, a new wave of software tools have appeared, building on top of these deep learning frameworks in order to accommodate modern probabilistic models containing DNNs (Tran et al., 2016; Cabañas et al., 2019; Tran et al., 2018; Bingham et al., 2018). These software tools usually fall under the umbrella term *probabilistic programming languages* (PPLs) (Gordon et al., 2014; Ghahramani, 2015), and provide support for methods for learning and reasoning about complex probabilistic models. Although PPLs have been present in the field of machine learning for many years, traditional PPLs have mainly focused on defining languages for expressing (more restricted types of) probabilistic models (Koller and Friedman, 2009) with only little focus on issues such as scalability. The advent of deep learning and the introduction of probabilistic models containing DNNs has motivated the development of a new family of PPLs offering support for flexible and complex models as well as scalable inference. Well-known examples include Edward2 (Tran et al., 2016, 2018), developed by Google and built on top of TensorFlow (Abadi et al., 2015), Pyro (Bingham et al., 2018) developed by Uber and built on top of Pytorch (Paszke et al., 2017), and PyMC3 (Salvatier et al., 2016) which is built on top of Theano (Bergstra et al., 2010).

The key data structure in these new PPLs are the so-called *stochastic computational graphs* (SCGs) (Schulman et al., 2015). SCGs extend standard *computational graphs* with stochastic nodes (represented as circles in the subsequent diagrams). The probability distributions associated with stochastic nodes are defined conditionally on their parents and enable the specification of complex functions involving expectations over random variables. Figure 6 (**Left**) shows an example of a simple SCG involving an expectation over a random variable z . Modern PPLs support a wide and diverse range of probability distributions for defining SCGs (Dillon et al., 2017). These probability distributions are defined over tensor objects to seamlessly accommodate the underlying CGs, which define operations over tensor objects too.

We note that SCGs are not directly implemented within PPLs, because computing the exact expected value of a complex function is typically infeasible. However, they are indirectly included through the use of a standard computational graph engine: Each stochastic node, z , is associated with a tensor, z^* , which represents a (set of) sample(s) from the distribution associated with z , and the generated samples can thus be fed to the underlying computational graph through the tensor z^* . Hence, SCGs can be *simulated* by sampling from the stochastic nodes and processing these samples by a standard CG. Figure 6 illustrates how SCG can be simulated using standard CGs. Note that CGs are designed to operate efficiently with tensors (current toolboxes like TensorFlow exploit high-performance computing hardware such as GPUs or TPUs (Abadi et al., 2015)), and it is therefore much more efficient to run the CG once over a collection of samples, rather than running the CG multiple times over a single sample.

In this way, SCGs can be used to define and support inference and learning of general probabilistic models, including the ones referenced in Section 4.1. More generally, all the concepts reviewed in this paper apply to any probabilistic model that can be defined by means of an SCG or which can be compiled into an equivalent SCG representation. For instance, the following model specification (illustrated by the top part in Figure 7) relating z with the natural parameters η_x of x can be equivalently represented by the SCG illustrated in the lower part of Figure 7.



$$h = \mathbb{E}_{z \sim \mathcal{N}(\mu, 1)}[(z - 5)^2] \quad \hat{h} = \frac{1}{k} \sum_{i=1}^k (z_i^* - 5)^2, \quad z_i^* \sim \mathcal{N}(\mu, 1)$$

Figure 6: **(Left)** A stochastic computational graph encoding the function $h = \mathbb{E}_z[(z - 5)^2]$, where $z \sim N(\mu, 1)$. **(Right)** Computational graph processing k samples from z and producing \hat{h} , an estimate of $\mathbb{E}_z[(z - 5)^2]$.

$$\begin{aligned}
\ln p(\boldsymbol{\beta}) &= \ln h(\boldsymbol{\beta}) + \boldsymbol{\alpha}^T t(\boldsymbol{\beta}) - a_g(\boldsymbol{\alpha}), \\
\ln p(\mathbf{z}_i | \boldsymbol{\beta}) &= \ln h(\mathbf{z}_i) + \eta_z(\boldsymbol{\beta})^T t(\mathbf{z}_i) - a_z(\eta_z(\boldsymbol{\beta})), \\
\mathbf{h}_0 &= \mathbf{r}_0(\mathbf{z}_i^T \boldsymbol{\beta}_0), \\
&\dots \\
\mathbf{h}_l &= \mathbf{r}_l(\mathbf{h}_{l-1}^T \boldsymbol{\beta}_l), \\
&\dots \\
\mathbf{h}_L &= \mathbf{r}_L(\mathbf{h}_L^T \boldsymbol{\beta}_L), \\
\ln p(\mathbf{x}_i | \mathbf{z}_i, \boldsymbol{\beta}) &= \ln h(\mathbf{x}_i) + \eta_x(\mathbf{h}_L)^T t(\mathbf{x}_i) - a_x(\eta_x(\mathbf{h}_L)). \tag{16}
\end{aligned}$$

From this example, we again see the main difference with respect to standard LVMs (see Section 2.1) is the conditional distribution of the observations \mathbf{x}_i given the local hidden variables \mathbf{z}_i and the global parameters $\boldsymbol{\beta}$, which is here governed by a DNN parameterized by $\boldsymbol{\beta}$.

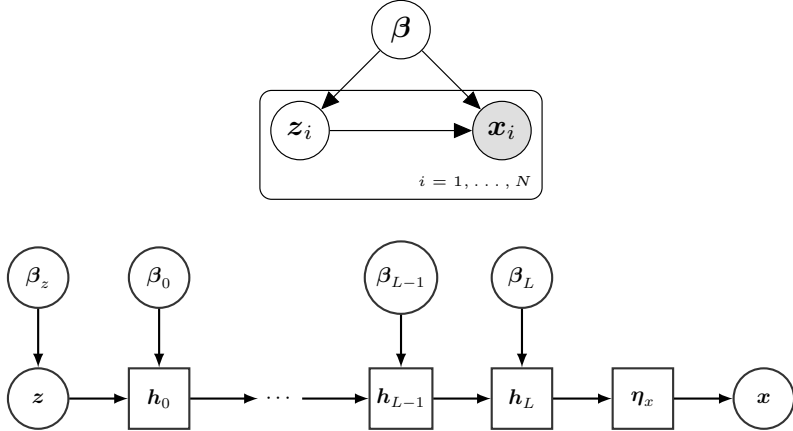


Figure 7: The top part depicts a probabilistic graphical model using plate notation (Koller and Friedman, 2009). The lower part depicts an abstract representation of a stochastic computational graph encoding the model, where the relation between z and x is defined by a DNN with $L + 1$ layers. See Section 4 for details.

5. Variational Inference with Deep Neural Networks

Similarly to standard probabilistic models, performing variational inference in deep latent variable models (as described in the previous section) also reduces to maximizing the ELBO function $\mathcal{L}(\lambda, \phi)$ given in Section 2.2 (Equation (8)); recall that this is equivalent to minimizing the KL divergence between the variational posterior $q(\beta, z|\beta, \phi)$ and the target distribution $p(\beta, z|x)$. However, as was also noted in the previous section, when the probabilistic model contains complex constructs like DNNs, it falls outside the conjugate exponential family and the traditional VI methods, tailored to this specific family form, can therefore not be applied.

In terms of the variational distribution, we will for the deep latent variable models considered in this section still assume the same factorization scheme defined in Equation (5). However, as we will see below, we need not adopt the conjugate models' strong restrictions on the variational approximation family (see Equation (6)). Instead, the only (and much weaker) restriction that we will impose is that *i*) the log probability of the variational distribution, $\ln q(\beta, z|\beta, \phi)$, can be represented by a computational graph (and, as a consequence, that it is differentiable wrt. β and ϕ) and *ii*) that we

can sample from the variational distribution $q(\beta, z|\beta, \phi)$. Depending on the specific method being applied, additional requirements may be introduced. The main methods currently available in the literature are introduced in the rest of this section.

5.1. Black Box Variational Inference

For the sake of presentation, we reparameterize the ELBO function with $r = (\beta, z)$ and $\nu = (\lambda, \phi)$ and define $g(r, \nu) = \ln p(x, r) - \ln q(r|\nu)$. With this notation the ELBO function \mathcal{L} of Equation (8) can be expressed as

$$\mathcal{L}(\nu) = \mathbb{E}_q[g(r, \nu)] = \int q(r|\nu)g(r, \nu)dr, \quad (17)$$

from which we see that the ELBO function can easily be represented by an SCG as shown in Figure 8. If the SCG in Figure 8 did not include stochastic nodes (thus corresponding to a standard CG), we could in principle perform variational inference (maximizing $\mathcal{L}(\nu)$ wrt. ν) by simply relying on automatic differentiation and a variation of gradient ascent. However, optimizing over SCGs is much more challenging because automatic differentiation does not readily apply. The problem is that the variational parameters ν (for which we should differentiate) also affects the expectation inherent in the ELBO function, see Equation (17):

$$\nabla_\nu \mathcal{L} = \nabla_\nu \mathbb{E}_q[g(r, \nu)]. \quad (18)$$

In the case of conjugate models, we could take advantage of their properties and derive closed-form solutions for this problem, as detailed in Section 2.2. In general, though, there are no closed-form solutions for computing gradients in non-conjugate models; a simple concrete example is the Bayesian logistic regression model (Murphy, 2012, Page 756).

In this section, we provide two generic solutions for computing the gradient of the ELBO function for probabilistic models including DNNs. Both methods directly rely on the automatic differentiation engines available for standard computational graphs. In this way, the methods can be seen as extending the automatic differentiation methods of standard computational graphs to SCGs, giving rise to a powerful approach to VI for generic probabilistic models. The main idea underlying both approaches is to compute

the gradient of the expectation given in Equation (18) using Monte Carlo techniques. More precisely, we will show how we can build unbiased estimates of this gradient by sampling from the variational (or an auxiliary) distribution without having to compute the gradient of the ELBO analytically (Ranganath et al., 2014; Wingate and Weber, 2013; Mnih and Gregor, 2014).

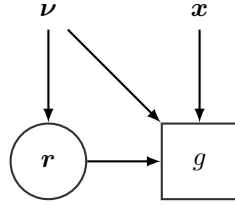


Figure 8: SCG representing the ELBO function $\mathcal{L}(\nu)$. r is distributed according to the variational distribution, $r \sim q(r|\nu)$.

5.1.1. Pathwise Gradients

The idea of this approach is to exploit reparameterizations of the variational distribution in terms of deterministic transformations of a noise distribution (Glasserman, 2013; Fu, 2006). A distribution $q(r|\nu)$ is reparameterizable if it can be expressed as

$$\begin{aligned} \epsilon &\sim q(\epsilon), \\ r &= t(\epsilon; \nu), \end{aligned} \tag{19}$$

where ϵ does not depend on parameter ν and $t(\cdot; \nu)$ is a deterministic function which encapsulates the dependence of r with respect to ν . This allows to compute any expectation over r as an expectation over ϵ . Exploiting this reparametrization property we can express the gradient of \mathcal{L} in Equation (18) as follows (Kingma and Welling, 2013;

Rezende et al., 2014; Titsias and Lázaro-Gredilla, 2014),

$$\begin{aligned}
\nabla_{\nu} \mathcal{L}(\boldsymbol{\nu}) &= \nabla_{\nu} \mathbb{E}_{\nu}[g(\mathbf{r}, \boldsymbol{\nu})] \\
&= \nabla_{\nu} \mathbb{E}_{\epsilon}[g(t(\epsilon; \boldsymbol{\nu}), \boldsymbol{\nu})] \\
&= \mathbb{E}_{\epsilon}[\nabla_{\nu} g(t(\epsilon; \boldsymbol{\nu}), \boldsymbol{\nu})] \\
&= \mathbb{E}_{\epsilon}[\nabla_{\nu} g(t(\epsilon; \boldsymbol{\nu}), \boldsymbol{\nu})^T \nabla_{\nu} t(\epsilon; \boldsymbol{\nu}) + \nabla_{\nu} g(t(\epsilon; \boldsymbol{\nu}), \boldsymbol{\nu})] \\
&= \mathbb{E}_{\epsilon}[\nabla_{\nu} g(\mathbf{r}, \boldsymbol{\nu})^T \nabla_{\nu} t(\epsilon; \boldsymbol{\nu}) + \nabla_{\nu} g(\mathbf{r}, \boldsymbol{\nu})] \\
&= \mathbb{E}_{\epsilon}[\nabla_{\nu} g(\mathbf{r}, \boldsymbol{\nu})^T \nabla_{\nu} t(\epsilon; \boldsymbol{\nu})].
\end{aligned} \tag{20}$$

Note that once we employ this reparameterization trick, the gradient can enter the expectation, something that could not happen with the score function gradient method. After that we simply apply the chain rule of derivatives. In the last step, we have taken into account that

$$\begin{aligned}
\mathbb{E}_{\epsilon}[\nabla_{\nu} g(\mathbf{r}, \boldsymbol{\nu})] &= \int \nabla_{\nu} g(\mathbf{r}, \boldsymbol{\nu}) q(\epsilon) d\epsilon \\
&= \int \nabla_{\nu} g(\mathbf{r}, \boldsymbol{\nu}) q(\mathbf{r} | \boldsymbol{\nu}) d\mathbf{r} \\
&= \mathbb{E}_q[\nabla_{\nu} g(\mathbf{r}, \boldsymbol{\nu})],
\end{aligned}$$

and since $g(\mathbf{r}, \boldsymbol{\nu}) = \ln p(\mathbf{x}, \mathbf{r}) - \ln q(\mathbf{r} | \boldsymbol{\nu})$ (and thus $\nabla_{\nu} g(\mathbf{r}, \boldsymbol{\nu}) = -\nabla_{\nu} \ln q(\mathbf{r} | \boldsymbol{\nu})$), and $\mathbb{E}_{\nu}[\nabla_{\nu} \ln q(\mathbf{r} | \boldsymbol{\nu})] = 0$, this term cancels out. The key advantage of this method is that the gradient estimator is informed by the gradient with respect to \mathbf{r} , which gives the direction of the maximum posterior mode.

Example 7 The Normal distribution is the best known example where this technique can be applied: A variable $w \sim \mathcal{N}(\mu, \sigma^2)$ can be reparameterized as $\epsilon \sim \mathcal{N}(0, 1)$ and $w = \mu + \sigma\epsilon$. So, exploiting this reparametrization we can compute the gradient of stochastic functions as the one defined in Figure 6, i.e. compute $\nabla_{\mu} \mathbb{E}_z[(z - 5)^2]$ where $z \sim \mathcal{N}(\mu, 1)$,

$$\nabla_{\mu} \mathbb{E}_z[(z - 5)^2] = \mathbb{E}_{\epsilon}[\nabla_{\mu}(\mu + \epsilon - 5)^2] = \mathbb{E}_{\epsilon}[2(\mu + \epsilon - 5)],$$

which can be easily approximated by a Monte Carlo sampling,

$$\nabla_{\mu} \mathbb{E}_z[(z - 5)^2] \approx \frac{1}{K} \sum_{i=1}^K 2(\mu + \epsilon_i - 5) \quad \epsilon_i \sim \mathcal{N}(0, 1).$$

In terms of an SCG, this approach can be applied by transforming the original SCG described in Figure 8 to the SCG described in Figure 9. Introducing this change, the underlying CG (as discussed in Figure 6) can be readily applied and employ automatic differentiation to get unbiased estimates of the gradients of the ELBO. In fact, we simply have to define a CG that computes a Monte Carlo estimation of function \mathcal{L} ,

$$\hat{\mathcal{L}} = \frac{1}{K} \sum_i^K \ln p(\mathbf{x}, t(\epsilon_i; \boldsymbol{\nu})) - \ln q(t(\epsilon_i; \boldsymbol{\nu}) | \boldsymbol{\nu}) \quad \epsilon_i \sim q(\epsilon) \quad (21)$$

and the derivations shown in Equation (20) are automatically performed by the automatic differentiation engine associated with the CG defining the above function. So, the user does not have to care about that.

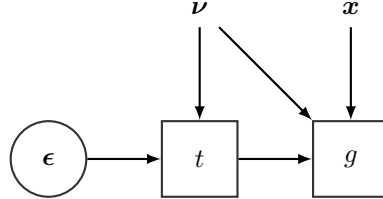


Figure 9: Reparameterized SCG representing the ELBO function $\mathcal{L}(\boldsymbol{\nu})$.

The problem with this approach is that only a few distributions can be reparameterized as shown in Equation (19). Fortunately, Figurnov et al. (2018) recently introduced an *implicit reparameterization approach* which apply to a wider range of distributions including Gamma, Beta, Dirichlet and von Misses. This method computes the gradient of \mathcal{L} as follows,

$$\nabla_{\boldsymbol{\nu}} \mathcal{L}(\boldsymbol{\nu}) = -\mathbb{E}_{\boldsymbol{\nu}} \left[\frac{\nabla_h g(\mathbf{r}, \boldsymbol{\nu})^T \nabla_{\boldsymbol{\nu}} F(\mathbf{r}; \boldsymbol{\nu})}{q(\mathbf{r} | \boldsymbol{\nu})} \right], \quad (22)$$

where $F(\mathbf{r}; \boldsymbol{\nu})$ is the cumulative distribution function of $q(\mathbf{r} | \boldsymbol{\nu})$. Other similar approaches have been proposed for models with discrete latent random variables (Tucker et al., 2017; Grathwohl et al., 2017).

This family of gradient estimators usually have lower variance than other methods (Kucukelbir et al., 2017) and they can even get good estimates using a single Monte Carlo sample in many cases. However, this algorithm requires the existence of the above explicit or implicit reparameterizations. Although many distributions can be covered by this method, there are other relevant distributions, as it is the case of the multinomial distribution, which can not be handled using any of these techniques.

Example 8 We continue with our running example about VAEs. In this case, we consider a VAE without an encoder network, which will be discussed in the next section. This model can be seen as a non-linear PCA model (the non-linearity is defined in terms of an ANN), described in Example 6. For this model, the ELBO function can be expressed as follows,

$$\begin{aligned}\mathcal{L}(\boldsymbol{\lambda}, \boldsymbol{\phi}) = & E_q[\ln p(\mathbf{x}|\mathbf{z}, \boldsymbol{\beta})] + E_q[\ln p(\mathbf{z})] + E_q[\ln p(\boldsymbol{\beta})] \\ & - E_q[\ln q(\mathbf{z}|\boldsymbol{\phi})] - E_q[\ln q(\boldsymbol{\beta}|\boldsymbol{\lambda})].\end{aligned}$$

Algorithm 4 shows the pseudo-code of the SCG defining the above ELBO function associated with this method using the pathwise trick. Look how we only use a single sample from the variational distribution q in reparameterized form. After that, the definition of the \mathcal{L} function is introduced, which includes the definition of the decoder network. So, gradients wrt variational parameters can be readily computed and optimized using standard algorithms. The output of this model in terms of dimensionality reduction were previously shown in Figure 5.

5.1.2. Score Function Gradients

This is a classic method for gradient estimation, also known as the REINFORCE gradient, (Ranganath et al., 2014; Glynn, 1990; Williams, 1992). It builds on the fol-

Algorithm 4 Pseudo-code of the function $\hat{\mathcal{L}}$ of a VAE without amortized inference (see Algorithm 3). We are using a single sample to compute the Monte Carlo estimation of $\hat{\mathcal{L}}$ (see Equation (21)). $\ln p_{\mathcal{N}}(\cdot|\cdot, \cdot)$ denotes the log-probability function of a Normal distribution.

input Data: \mathbf{x}_{train} , Variational Parameters: $\boldsymbol{\lambda}, \boldsymbol{\phi}$

Sample (using reparameterization) from $q(\boldsymbol{\beta}|\boldsymbol{\lambda})$ and $q(\mathbf{z}|\boldsymbol{\phi})$.

$$\epsilon_{\alpha_0}, \epsilon_{\beta_0}, \epsilon_{\alpha_1}, \epsilon_{\beta_1}, \epsilon_z \sim \mathcal{N}(\mathbf{0}, \mathbf{I})$$

$$\boldsymbol{\alpha}_0 = \boldsymbol{\lambda}_{\alpha_0, \mu} + \epsilon_{\alpha_0} \boldsymbol{\lambda}_{\alpha_0, \sigma}, \quad \boldsymbol{\beta}_0 = \boldsymbol{\lambda}_{\beta_0, \mu} + \epsilon_{\beta_0} \boldsymbol{\lambda}_{\beta_0, \sigma}$$

$$\boldsymbol{\alpha}_1 = \boldsymbol{\lambda}_{\alpha_1, \mu} + \epsilon_{\alpha_1} \boldsymbol{\lambda}_{\alpha_1, \sigma}, \quad \boldsymbol{\beta}_1 = \boldsymbol{\lambda}_{\beta_1, \mu} + \epsilon_{\beta_1} \boldsymbol{\lambda}_{\beta_1, \sigma}$$

$$\mathbf{z} = \boldsymbol{\phi}_{z, \mu} + \epsilon_z \boldsymbol{\phi}_{z, \sigma}$$

Pass the variational sample \mathbf{z} through the decoder ANN

$$\mathbf{h}_0 = \text{relu}(\mathbf{z}\boldsymbol{\beta}_0^T + \boldsymbol{\alpha}_0)$$

$$\boldsymbol{\mu}_x = \mathbf{h}_0 \boldsymbol{\beta}_1^T + \boldsymbol{\alpha}_1$$

Define the “energy part” of the ELBO function $E_q[\ln p(\mathbf{x}_{train}, \mathbf{z}, \boldsymbol{\alpha}, \boldsymbol{\beta})]$.

$$\mathcal{L} = \ln p_{\mathcal{N}}(\mathbf{x}_{train}|\boldsymbol{\mu}_x, \sigma_x^2 \mathbf{I})$$

$$\mathcal{L} = \mathcal{L} + \ln p_{\mathcal{N}}(\mathbf{z}|\mathbf{0}, \mathbf{I}) + \sum_i \ln p_{\mathcal{N}}(\boldsymbol{\alpha}_i|\mathbf{0}, \mathbf{I}) + \ln p_{\mathcal{N}}(\boldsymbol{\beta}_i|\mathbf{0}, \mathbf{I})$$

Define the “entropy part” of the ELBO function $E_q[\ln q(\mathbf{z}, \boldsymbol{\alpha}, \boldsymbol{\beta})]$.

$$\mathcal{L} = \mathcal{L} - \ln p_{\mathcal{N}}(\mathbf{z}|\boldsymbol{\phi}_{z, \mu}, \boldsymbol{\phi}_{z, \sigma}^2)$$

$$\mathcal{L} = \mathcal{L} - \sum_i \ln p_{\mathcal{N}}(\boldsymbol{\alpha}_i|\boldsymbol{\lambda}_{\alpha_i, \mu}, \boldsymbol{\lambda}_{\alpha_i, \sigma}^2) + \ln p_{\mathcal{N}}(\boldsymbol{\beta}_i|\boldsymbol{\lambda}_{\beta_i, \mu}, \boldsymbol{\lambda}_{\beta_i, \sigma}^2)$$

return \mathcal{L}

lowing generic transformations to compute the gradient of an expected value,

$$\begin{aligned} \nabla_{\boldsymbol{\nu}} \mathcal{L}(\boldsymbol{\nu}) &= \nabla_{\boldsymbol{\nu}} \int q(\mathbf{r}|\boldsymbol{\nu}) g(\mathbf{r}, \boldsymbol{\nu}) d\mathbf{r} \\ &= \int \nabla_{\boldsymbol{\nu}} q(\mathbf{r}|\boldsymbol{\nu}) g(\mathbf{r}, \boldsymbol{\nu}) + q(\mathbf{r}|\boldsymbol{\nu}) \nabla_{\boldsymbol{\nu}} g(\mathbf{r}, \boldsymbol{\nu}) d\mathbf{r} \\ &= \int q(\mathbf{r}|\boldsymbol{\nu}) \nabla_{\boldsymbol{\nu}} \ln q(\mathbf{r}|\boldsymbol{\nu}) g(\mathbf{r}, \boldsymbol{\nu}) + q(\mathbf{r}|\boldsymbol{\nu}) \nabla_{\boldsymbol{\nu}} g(\mathbf{r}, \boldsymbol{\nu}) d\mathbf{r} \\ &= \mathbb{E}_{\boldsymbol{\nu}} [\nabla_{\boldsymbol{\nu}} \ln q(\mathbf{r}|\boldsymbol{\nu}) g(\mathbf{r}, \boldsymbol{\nu}) + \nabla_{\boldsymbol{\nu}} g(\mathbf{r}, \boldsymbol{\nu})]. \end{aligned} \tag{23}$$

As $\mathbb{E}_\nu[\nabla_\nu g(\mathbf{r}, \boldsymbol{\nu})] = \mathbb{E}_\nu[\nabla_\nu \ln q(\mathbf{r}|\boldsymbol{\nu})] = 0$ ³, the gradient of the ELBO simplifies to,

$$\nabla_\nu \mathcal{L}(\boldsymbol{\nu}) = \mathbb{E}_\nu[\nabla_\nu \ln q(\mathbf{r}|\boldsymbol{\nu})g(\mathbf{r}, \boldsymbol{\nu})]. \quad (24)$$

From the above equation, we can obtain unbiased estimates of the gradient by sampling from $q(\mathbf{r}|\boldsymbol{\nu})$. This method is fairly general because it only requires evaluating the function $g(\mathbf{r}, \boldsymbol{\nu})$ and computing the gradient for the variational approximation, $\nabla_\nu \ln q(\mathbf{r}|\boldsymbol{\nu})$. In consequence, it applies to a really wide range of models including those ones already covered by *pathwise gradients*. However, this algorithm may easily yield high variance estimates of the gradients when the dimension of $\boldsymbol{\nu}$ is relatively high. So, it may require the use of variance reduction techniques to make it work successfully (Ruiz et al., 2016; Ranganath et al., 2014; Titsias and Lázaro-Gredilla, 2014; Mnih and Rezende, 2016). In practical settings, one should only resort to this method when the *pathwise gradients* estimators are not applicable.

Example 9 We revisit Example 7. We have to compute the gradient of an expectation $\nabla_\mu \mathbb{E}_z[(z-5)^2]$, where $z \sim \mathcal{N}(\mu, 1)$. Applying score function gradients, this could be computed as follows,

$$\begin{aligned} \nabla_\mu \mathbb{E}_z[(z-5)^2] &= \mathbb{E}_\mu[(z-5)^2 \nabla_\mu \ln N(z|\mu, 1)] \\ &= \mathbb{E}_\mu[(z-5)^2 \nabla_\mu(-0.5(z-\mu)^2)] \\ &= \mathbb{E}_\mu[(z-5)^2(\mu-z)], \end{aligned}$$

which can be easily approximated by a Monte Carlo sampling,

$$\nabla_\mu \mathbb{E}_z[(z-5)^2] \approx \frac{1}{K} \sum_{i=1}^K (z_i - 5)^2(\mu - z_i) \quad z_i \sim \mathcal{N}(\mu, 1).$$

In terms of SCG, this trick can be implemented following the indications given by Foerster et al. (2018). The main idea is to transform the CG in such a way that when automatic differentiation is applied to the underlying CG, we return the unbiased

³See the discussion right after Equation (20).

estimates provided by Equation (24). This is done by defining a SCG encoding the following definition of the ELBO function,

$$\mathcal{L}(\boldsymbol{\nu}) = E_{stop[q]}[g(\mathbf{r}, \boldsymbol{\nu})e^{\ln q(\mathbf{r}|\boldsymbol{\nu}) - stop[\ln q(\mathbf{r}|\boldsymbol{\nu})]}], \quad (25)$$

where $stop[\cdot]$ is a special function usually provided by automatic differentiation engines to stop the recursive application of the derivative rules in some parts of the CG. $stop[\cdot]$ behaves like the identity function, i.e. $stop[x] = x$, when evaluated, but it behaves like a constant when derivating, i.e. $\nabla_x stop[x]f(x) = x\nabla_x f(x)$ and $\nabla_x stop[x] = 0$. In that way, the gradient of $\mathcal{L}(\boldsymbol{\nu})$ is computed as

$$\begin{aligned} \nabla_{\boldsymbol{\nu}} \mathcal{L}(\boldsymbol{\nu}) &= E_q[\nabla_{\boldsymbol{\nu}} g(\mathbf{r}, \boldsymbol{\nu})e^{\ln q(\mathbf{r}|\boldsymbol{\nu}) - stop[\ln q(\mathbf{r}|\boldsymbol{\nu})]} \\ &\quad + g(\mathbf{r}, \boldsymbol{\nu})\nabla_{\boldsymbol{\nu}}(e^{\ln q(\mathbf{r}|\boldsymbol{\nu}) - stop[\ln q(\mathbf{r}|\boldsymbol{\nu})]})] \\ &= E_q[\nabla_{\boldsymbol{\nu}} g(\mathbf{r}, \boldsymbol{\nu}) + g(\mathbf{r}, \boldsymbol{\nu})\nabla_{\boldsymbol{\nu}}(\ln q(\mathbf{r}|\boldsymbol{\nu}) - stop[\ln q(\mathbf{r}|\boldsymbol{\nu})])] \\ &= E_q[\nabla_{\boldsymbol{\nu}} \ln q(\mathbf{u}|\boldsymbol{\nu}) + g(\mathbf{r}, \boldsymbol{\nu})\nabla_{\boldsymbol{\nu}} \ln q(\mathbf{r}|\boldsymbol{\nu})] \\ &= E_q[g(\mathbf{r}, \boldsymbol{\nu})\nabla_{\boldsymbol{\nu}} \ln q(\mathbf{r}|\boldsymbol{\nu})]. \end{aligned}$$

5.2. ELBO optimization with Amortized Variational Inference

In principle, we can address the optimization of the ELBO function using an off-the-shelf gradient ascent algorithm with the techniques presented in the previous section. The ELBO function $\mathcal{L}(\boldsymbol{\lambda}, \boldsymbol{\phi})$ should now be expressed again in terms of global variational parameters, $\boldsymbol{\lambda}$, defining the variational distribution over the global latent variables $q(\boldsymbol{\beta}|\boldsymbol{\lambda})$; and in terms of local variational parameters, $\boldsymbol{\phi}$, defining the variational distribution over the local latent variables $q(\mathbf{z}|\boldsymbol{\phi})$. Note that we still assume that our variational posterior fully factorizes as shown in Equation (5). The case where both reparameterizable and non-reparameterizable random variables coexist in the model can be easily handled by transforming the local parts of the SCG affecting those random variables as shown in the previous section.

However, $\boldsymbol{\phi}$ is a parameter vector that grows with the data, $\boldsymbol{\phi} = (\phi_1, \dots, \phi_N)$, giving rise to an optimization problem which can not be handled when the model involves big data sets.

To address these scenarios we can rely on some of the tricks detailed in Section 2.3. First, we can reparameterize $\mathcal{L}(\boldsymbol{\lambda}, \boldsymbol{\phi})$ only in terms of $\boldsymbol{\lambda}$, as previously shown in Equations (11) and (12),

$$\mathcal{L}(\boldsymbol{\lambda}) = \mathbb{E}_q[\ln p(\boldsymbol{\beta})] - \mathbb{E}_q[\ln q(\boldsymbol{\beta}|\boldsymbol{\lambda})] + \sum_{i=1}^N \max_{\boldsymbol{\phi}_i} (\mathbb{E}_q[\ln p(\mathbf{x}_i, \mathbf{z}_i|\boldsymbol{\beta})] - \mathbb{E}_q[\ln q(\mathbf{z}_i|\boldsymbol{\phi}_i)]).$$

As done in Section 2.3, we can get unbiased noisy estimates of this ELBO by data subsampling. Let be I a randomly chosen index, $I \in \{1, \dots, N\}$, and

$$\mathcal{L}_I(\boldsymbol{\lambda}) = \mathbb{E}_q[\ln p(\boldsymbol{\beta})] - \mathbb{E}_q[\ln q(\boldsymbol{\beta}|\boldsymbol{\lambda})] + N \max_{\boldsymbol{\phi}_I} (\mathbb{E}_q[\ln p(\mathbf{x}_I, \mathbf{z}_I|\boldsymbol{\beta})] - \mathbb{E}_q[\ln q(\mathbf{z}_I|\boldsymbol{\phi}_I)]).$$

It is clear, that the expectation of $\mathcal{L}_I(\boldsymbol{\lambda})$ is equal to $\mathcal{L}(\boldsymbol{\lambda})$. Then, computing the gradient of $\mathcal{L}_I(\boldsymbol{\lambda})$ wrt to $\boldsymbol{\lambda}$ will give us a noisy unbiased estimate of the gradient. However, in this case, it would require to solve a maximization problem for each subsampled data point (i.e. $\max_{\boldsymbol{\phi}_I}$). In the case of conjugate exponential models, this inner maximization step can be computed in closed form, as shown in Equation (10). But now, doing that using an iterative algorithm, based on the methods described in Section 5.1, would be infeasible.

Amortized inference (Dayan et al., 1995; Gershman and Goodman, 2014) solves this problem by learning a mapping function, denoted by \mathbf{s} , between \mathbf{x}_i and $\boldsymbol{\phi}_i$ parameterized by $\boldsymbol{\theta}$, i.e. $\boldsymbol{\phi}_i = \mathbf{s}(\mathbf{x}_i|\boldsymbol{\theta})$. Hence, $\mathcal{L}_I(\boldsymbol{\lambda})$ is expressed as $\mathcal{L}_I(\boldsymbol{\lambda}, \boldsymbol{\theta})$,

$$\begin{aligned} \mathcal{L}_I(\boldsymbol{\lambda}, \boldsymbol{\theta}) &= \mathbb{E}_q[\ln p(\boldsymbol{\beta})] - \mathbb{E}_q[\ln q(\boldsymbol{\beta}|\boldsymbol{\lambda})] \\ &+ N \cdot \mathbb{E}_q[\ln p(\mathbf{x}_I, \mathbf{z}_I|\boldsymbol{\beta})] - N \cdot \mathbb{E}_q[\ln q(\mathbf{z}_I|\mathbf{x}_I, \boldsymbol{\phi}_I = \mathbf{s}(\mathbf{x}_I|\boldsymbol{\theta}))]. \end{aligned}$$

The parameter vector $\boldsymbol{\theta}$ is shared among all the data points and does not grow with the data set as happened with $\boldsymbol{\phi} = \{\boldsymbol{\phi}_1, \dots, \boldsymbol{\phi}_N\}$. On the other hand, amortized inference assumes that the parameterized function \mathbf{s} is flexible enough to allow the prediction of the local variational parameters $\boldsymbol{\phi}_i$ from the data points \mathbf{x}_i . But, in any case, the family of variational distributions defined by this technique,

$$q(\boldsymbol{\beta}, \mathbf{z}|\mathbf{x}, \boldsymbol{\lambda}, \boldsymbol{\theta}) = q(\boldsymbol{\beta}|\boldsymbol{\lambda}) \prod_{i=1}^N q(\mathbf{z}_i|\mathbf{x}_i, \boldsymbol{\phi}_i = \mathbf{s}(\mathbf{x}_i|\boldsymbol{\theta})),$$

is more restricted than the one defined in Equation (5), which directly depends of λ and ϕ . So, there is a trade-off between flexibility in the variational approximation and computational efficiency when applying amortized inference techniques.

Note that the amortized function greatly simplifies the use of the model when making predictions over unseen data x' . If we need to compute the posterior $p(z'|x')$ over a new data sample (e.g. for dimensionality reduction when using a VAE model), we just need to invoke the learnt amortized inference function to recover this posterior, $q(z'|z = s(x'|\theta^*))$.

An unbiased estimate of the gradient of $\mathcal{L}_I(\lambda, \theta)$ wrt to λ and θ can be computed using the techniques described in the previous section, as both affect an expectation term. Note that the unbiased estimate of the gradient of $\mathcal{L}_I(\lambda, \theta)$ is also an unbiased estimate of the gradient of $\mathcal{L}(\lambda, \theta)$. Similarly to Equation (13), the ELBO can be maximized by following noisy estimates of the gradient,

$$\begin{aligned}\lambda_{t+1} &= \lambda_t + \rho_t \hat{\nabla}_\lambda \mathcal{L}_{I_t}(\lambda_t, \theta_t), \\ \theta_{t+1} &= \theta_t + \rho_t \hat{\nabla}_\theta \mathcal{L}_{I_t}(\lambda_t, \theta_t)\end{aligned}\tag{26}$$

where I_t is the index of the data point randomly subsampled at time step t .

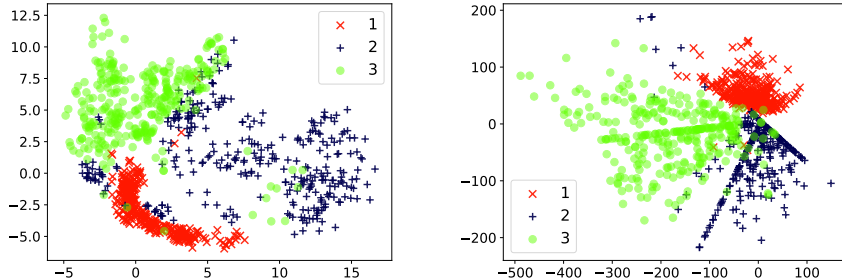


Figure 10: 2-dimensional latent representation of the the MNIST dataset resulting of applying: **(Left)** a non-linear probabilistic PCA, and **(Right)** a VAE. The ANNs of the non-linear PCA and the ones defining the VAE’s decoder and encoder contain a single hidden layer of size 100.

Example 10 We can finally arrive at the original formulation of VAEs, which includes an amortized inference function linking the data samples

with the latent variables \mathbf{z} . This amortized function takes the form of a neural network, and it is known in the literature as the *encoder network*, because it translates an observation \mathbf{x} to (a distribution over) its hidden representation \mathbf{z} . The other neural network of the model, known in the literature as the *decoder network*, links the latent variable \mathbf{z} to (a distribution over) the observable variable \mathbf{x} . The existence of this two networks, the encoder and the decoder, establishes a direct link with the previously known auto-encoder networks (Hinton and Salakhutdinov, 2006). In this example, both the encoder and the decoder network have a single hidden layer with a relu activation function.

Algorithm 4 shows the pseudo-code to define the ELBO function associated with this method using the pathwise trick. Again, in first place, we define and sample from the variational distribution q in reparameterized form. For defining this variational distribution, we need to introduce the encoder network, which helps to sample from the variational distribution over \mathbf{z}_I given \mathbf{x}_I . Similarly to the previous example, we end up defining the \mathcal{L}_I function, which includes the definition of the decoder network. Again, this pseudo-code also defines at the same time the underlying computational graph. So, gradients wrt variational parameters can be readily computed and optimized using, in this case, stochastic gradient ascent or some of its variations.

Figure 10 shows the result of the application of this VAE over a reduced MNIST data set containing three digits. These results show how the VAE is also able to separate these three classes. Figure 11 shows the evolution of the ELBO during the optimization process (using Adam Optimizer with learning rate equal to 0.01), and compared with the evolution of the ELBO of the non-linear probabilistic PCA model of Example 6. Remind that this last model is like a VAE without encoder network. In consequence, this PCA like model can not be optimized using a stochastic gradient ascent algorithm. The consequence is that the ELBO grows more slowly and that

Algorithm 5 Pseudo-code of the function \mathcal{L}_I of a Variational Auto-encoder. We are using a single sample to compute the Monte Carlo estimation of $\hat{\mathcal{L}}$ (see Equation (21)). $\ln p_{\mathcal{N}}(\cdot | \cdot, \cdot)$ denotes the log-probability function of a Normal distribution.

input Data: \mathbf{x}_I a single data-sample, N size of the data, Variational Parameters: $\boldsymbol{\lambda}, \boldsymbol{\theta}$

```

# Sample (using reparametrization) from  $q(\boldsymbol{\beta}|\boldsymbol{\lambda})$ .
 $\epsilon_{\theta_0}, \epsilon_{\theta'_0}, \epsilon_{\theta_1}, \epsilon_{\theta'_1} \sim \mathcal{N}(\mathbf{0}, \mathbf{I})$ 
 $\boldsymbol{\theta}_0 = \boldsymbol{\lambda}_{\theta_0, \mu} + \epsilon_{\theta_0} \boldsymbol{\lambda}_{\theta_0, \sigma}, \quad \boldsymbol{\theta}'_0 = \boldsymbol{\lambda}_{\theta'_0, \mu} + \epsilon_{\theta'_0} \boldsymbol{\lambda}_{\theta'_0, \sigma}$ 
 $\boldsymbol{\theta}_1 = \boldsymbol{\lambda}_{\theta_1, \mu} + \epsilon_{\theta_1} \boldsymbol{\lambda}_{\theta_1, \sigma}, \quad \boldsymbol{\theta}'_1 = \boldsymbol{\lambda}_{\theta'_1, \mu} + \epsilon_{\theta'_1} \boldsymbol{\lambda}_{\theta'_1, \sigma}$ 
# Pass  $\mathbf{x}$  through the encoder network and sample  $\mathbf{z}_I \sim q(\mathbf{z}|\boldsymbol{\phi} = \mathbf{s}(\mathbf{x}_I|\boldsymbol{\theta}))$ 
 $\mathbf{h}_{z,0} = \text{relu}(\mathbf{x}_I \boldsymbol{\theta}_0^T + \boldsymbol{\theta}'_0)$ 
 $\mathbf{h}_{z,1} = \mathbf{h}_{z,0} \boldsymbol{\theta}_1^T + \boldsymbol{\theta}'_1$ 
#  $\mathbf{h}_{z,1}$  contains both the mean,  $\mathbf{h}_{z,1, \mu}$ , and the scale,  $\mathbf{h}_{z,1, \sigma}$ .
 $\epsilon_z \sim \mathcal{N}(\mathbf{0}, \mathbf{I})$ 
 $\mathbf{z}_I = \mathbf{h}_{z,1, \mu} + \epsilon_z \mathbf{h}_{z,1, \sigma}$ 
# Pass the variational sample  $\mathbf{z}$  through the decoder network
 $\epsilon_{\alpha_0}, \epsilon_{\beta_0}, \epsilon_{\alpha_1}, \epsilon_{\beta_1} \sim \mathcal{N}(\mathbf{0}, \mathbf{I})$ 
 $\boldsymbol{\alpha}_0 = \boldsymbol{\lambda}_{\alpha_0, \mu} + \epsilon_{\alpha_0} \boldsymbol{\lambda}_{\alpha_0, \sigma}, \quad \boldsymbol{\beta}_0 = \boldsymbol{\lambda}_{\beta_0, \mu} + \epsilon_{\beta_0} \boldsymbol{\lambda}_{\beta_0, \sigma}$ 
 $\boldsymbol{\alpha}_1 = \boldsymbol{\lambda}_{\alpha_1, \mu} + \epsilon_{\alpha_1} \boldsymbol{\lambda}_{\alpha_1, \sigma}, \quad \boldsymbol{\beta}_1 = \boldsymbol{\lambda}_{\beta_1, \mu} + \epsilon_{\beta_1} \boldsymbol{\lambda}_{\beta_1, \sigma}$ 
 $\mathbf{h}_0 = \text{relu}(\mathbf{z}_I \boldsymbol{\beta}_0^T + \boldsymbol{\alpha}_0)$ 
 $\boldsymbol{\mu}_x = \mathbf{h}_0 \boldsymbol{\beta}_1^T + \boldsymbol{\alpha}_1$ 
# Define the “energy part” of the ELBO function
 $\mathcal{L}_I = N \cdot \ln p_{\mathcal{N}}(\mathbf{x}_I | \boldsymbol{\mu}_x, \sigma_x^2 \mathbf{I}) + N \cdot \ln p_{\mathcal{N}}(\mathbf{z}_I | \mathbf{0}, \mathbf{I})$ 
 $\mathcal{L}_I = \mathcal{L}_I + \sum_i \ln p_{\mathcal{N}}(\boldsymbol{\alpha}_i | \mathbf{0}, \mathbf{I}) + \ln p_{\mathcal{N}}(\boldsymbol{\beta}_i | \mathbf{0}, \mathbf{I})$ 
# Define the “entropy part” of the ELBO function
 $\mathcal{L}_I = \mathcal{L}_I - N \cdot \ln p_{\mathcal{N}}(\mathbf{z}_I | \mathbf{h}'_{1, \mu}, \mathbf{h}'_{1, \sigma})$ 
 $\mathcal{L}_I = \mathcal{L}_I - \sum_i \ln p_{\mathcal{N}}(\boldsymbol{\alpha}_i | \boldsymbol{\lambda}_{\alpha_i, \mu}, \boldsymbol{\lambda}_{\alpha_i, \sigma}^2) + \ln p_{\mathcal{N}}(\boldsymbol{\beta}_i | \boldsymbol{\lambda}_{\beta_i, \mu}, \boldsymbol{\lambda}_{\beta_i, \sigma}^2)$ 
return  $\mathcal{L}_I$ 

```

the method is not scalable.

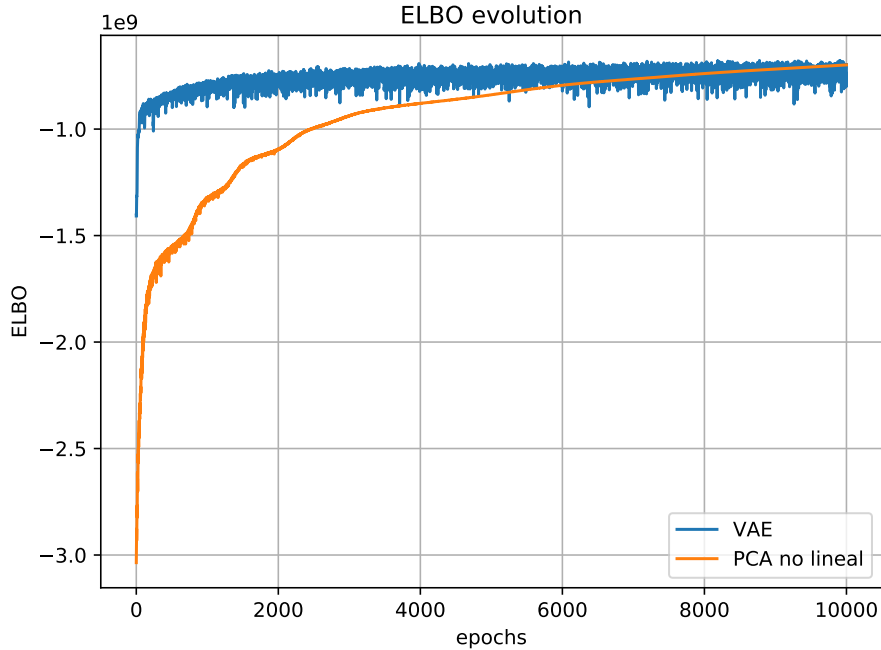


Figure 11: Evolution of the ELBO for the VAE of Example 10 (with a mini-batch size of 100 samples) and the non-linear probabilistic PCA introduced in Example 6. The latter model is equivalent to the former but without amortized inference network.

6. Conclusions and Open Issues

In this paper we have discussed the recent breakthroughs in approximate inference for PGMs. In particular, we have considered variational inference, a scalable and versatile approach for doing approximate inference in probabilistic models, that allows the data analyst to build flexible models, without enforcing explicit modelling assumptions (e.g. linear relationship between random variables) VI has a sound mathematical foundation that is well understood, and the approach has good theoretical properties. For instance, VI is (in theory) guaranteed to converge to the approximate posterior q from a set of viable approximations \mathcal{Q} that is the (local) maximum of the ELBO, as defined in Equation (8). Nevertheless, variational inference often encounter difficulties when used in practice. Random initialization of the parameter search can have a pronounced

effect on the end-result, and unless extra care is taken, issues wrt. numerical stability may also endanger the robustness of the obtained results. More research is needed to develop practical guidelines for using variational inference.

As the power of deep neural networks have entered PGMs, the PGM community has largely responded enthusiastically, embracing the new extensions to the PGM toolbox, and used it eagerly. This has lead to new and interesting tools and models, some of which are discussed in this paper. However, we also see a potential pitfall here: The trend is to move away from the modelling paradigm that the PGM community traditionally held so high, and move towards catch-all LVMs (like the one depicted in Figure 1). These models “*let the data speak for itself*”, but at the cost of interpretability. PGMs used to be regarded as fully transparent models, but become more opaque as less effort is put into modelling, and more is put on general purpose inference techniques. Initial steps have already been made to leverage the PGM’s modelling power also in this context (see, e.g., Kingma et al. (2014)), but a seamless integration of neural networks and PGMs to leverage flexibility of DNNs to model local CPTs requires further developments: In a PGM model where some variables are defined using traditional probability distributions and others use deep neural networks, parts of the model may lend itself to efficient approximative inference (e.g., using VMP as described in Section 2.4), while others do not. An inference engine that utilizes an efficient (mixed) strategy for approximate inference in such models, would be a valuable contribution. Secondly, VI solves the inference problem by solving a continuous optimization problem. However, this is insufficient if the model contains latent categorical variables. While some PPL, like the current release⁴ of Pyro, (Bingham et al., 2018), implements automatic enumeration over discrete latent variables, alternative approaches like the Concrete distribution (Maddison et al., 2016) is gaining some ground. Thirdly, focusing more on the modelling allows for a balancing between approximations in the *inference* vs. exact inference after making approximations in the *modelling*. Here, the modelling approach may lead to be better understood approximations, and therefore give results that are more robust and better suited for decision support.

⁴Pyro version 0.3.4.

Acknowledgements

This research has been partly funded by the Spanish Ministry of Science, Innovation and Universities, through projects TIN2015-74368-JIN, TIN2016-77902-C3-3-P and by ERDF funds.

References

Abadi M, Agarwal A, Barham P, Brevdo E, Chen Z, Citro C, Corrado GS, Davis A, Dean J, Devin M, Ghemawat S, Goodfellow I, Harp A, Irving G, Isard M, Jia Y, Jozefowicz R, Kaiser L, Kudlur M, Levenberg J, Mané D, Monga R, Moore S, Murray D, Olah C, Schuster M, Shlens J, Steiner B, Sutskever I, Talwar K, Tucker P, Vanhoucke V, Vasudevan V, Viégas F, Vinyals O, Warden P, Wattenberg M, Wicke M, Yu Y, Zheng X. TensorFlow: Large-scale machine learning on heterogeneous systems. 2015. URL: <http://tensorflow.org/>; software available from tensorflow.org.

Amari SI. Natural gradient works efficiently in learning. *Neural computation* 1998;10(2):251–76.

Barndorff-Nielsen O. Information and exponential families: in statistical theory. John Wiley & Sons, 2014.

Bergstra J, Breuleux O, Bastien F, Lamblin P, Pascanu R, Desjardins G, Turian J, Warde-Farley D, Bengio Y. Theano: a CPU and GPU math expression compiler. In: Proceedings of the Python for scientific computing conference (SciPy). Austin, TX; volume 4; 2010. .

Bingham E, Chen JP, Jankowiak M, Obermeyer F, Pradhan N, Karaletsos T, Singh R, Szerlip P, Horsfall P, Goodman ND. Pyro: Deep universal probabilistic programming. arXiv preprint arXiv:181009538 2018;.

Bishop CM. Latent variable models. In: Learning in graphical models. Springer; 1998. p. 371–403.

Bishop CM. Pattern recognition and machine learning. Springer, 2006.

Blei DM. Build, compute, critique, repeat: Data analysis with latent variable models. *Annual Review of Statistics and Its Application* 2014;1:203–32.

Blei DM, Ng AY, Jordan MI. Latent dirichlet allocation. *Journal of machine Learning research* 2003;3(Jan):993–1022.

Bottou L. Large-scale machine learning with stochastic gradient descent. In: *Proceedings of COMPSTAT'2010*. Springer; 2010. p. 177–86.

Cabañas R, Salmerón A, Masegosa AR. Inferpy: Probabilistic modeling with tensorflow made easy. *Knowledge-Based Systems* 2019;.

Card D, Tan C, Smith NA. A neural framework for generalized topic models. *arXiv preprint arXiv:170509296* 2017;.

Chen T, Li M, Li Y, Lin M, Wang N, Wang M, Xiao T, Xu B, Zhang C, Zhang Z. Mxnet: A flexible and efficient machine learning library for heterogeneous distributed systems. *arXiv preprint arXiv:151201274* 2015;.

Chung J, Kastner K, Dinh L, Goel K, Courville AC, Bengio Y. A recurrent latent variable model for sequential data. In: *Advances in neural information processing systems*. 2015. p. 2980–8.

Dayan P, Hinton GE, Neal RM, Zemel RS. The helmholtz machine. *Neural computation* 1995;7(5):889–904.

Dillon JV, Langmore I, Tran D, Brevdo E, Vasudevan S, Moore D, Patton B, Alemi A, Hoffman M, Saurous RA. Tensorflow distributions. *arXiv preprint arXiv:171110604* 2017;.

Doersch C. Tutorial on variational autoencoders. *arXiv preprint arXiv:160605908* 2016;.

Figurnov M, Mohamed S, Mnih A. Implicit reparameterization gradients. *arXiv preprint arXiv:180508498* 2018;.

Fisher RA. The use of multiple measurements in taxonomic problems. *Annals of eugenics* 1936;7(2):179–88.

Foerster J, Farquhar G, Al-Shedivat M, Rocktäschel T, Xing EP, Whiteson S. Dice: The infinitely differentiable Monte-Carlo estimator. arXiv preprint arXiv:180205098 2018;.

Fu MC. Gradient estimation. *Handbooks in operations research and management science* 2006;13:575–616.

Gershman S, Goodman N. Amortized inference in probabilistic reasoning. In: *Proceedings of the Annual Meeting of the Cognitive Science Society*. volume 36; 2014.

Ghahramani Z. Probabilistic machine learning and artificial intelligence. *Nature* 2015;521(7553):452.

Gilks WR, Richardson S, Spiegelhalter D. *Markov chain Monte Carlo in practice*. Chapman and Hall/CRC, 1995.

Glasserman P. *Monte Carlo methods in financial engineering*. volume 53. Springer Science & Business Media, 2013.

Glynn PW. Likelihood ratio gradient estimation for stochastic systems. *Communications of the ACM* 1990;33(10):75–84.

Gómez-Bombarelli R, Wei JN, Duvenaud D, Hernández-Lobato JM, Sánchez-Lengeling B, Sheberla D, Aguilera-Iparraguirre J, Hirzel TD, Adams RP, Aspuru-Guzik A. Automatic chemical design using a data-driven continuous representation of molecules. *ACS central science* 2018;4(2):268–76.

Goodfellow I, Bengio Y, Courville A, Bengio Y. *Deep learning*. MIT press Cambridge, 2016.

Goodfellow I, Pouget-Abadie J, Mirza M, Xu B, Warde-Farley D, Ozair S, Courville A, Bengio Y. Generative adversarial nets. In: *Advances in neural information processing systems*. 2014. p. 2672–80.

Gordon AD, Henzinger TA, Nori AV, Rajamani SK. Probabilistic programming. In: Proceedings of the on Future of Software Engineering. ACM; 2014. p. 167–81.

Grathwohl W, Choi D, Wu Y, Roeder G, Duvenaud D. Backpropagation through the void: Optimizing control variates for black-box gradient estimation. arXiv preprint arXiv:171100123 2017;.

Gregor K, Danihelka I, Graves A, Rezende DJ, Wierstra D. Draw: A recurrent neural network for image generation. arXiv preprint arXiv:150204623 2015;.

Griewank A. On automatic differentiation. Mathematical Programming: recent developments and applications 1989;6(6):83–107.

Hastie T, Tibshirani R, Friedman J. The Elements of Statistical Learning. New York, NY, USA: Springer New York Inc., 2001.

Hinton GE. Deep belief networks. Scholarpedia 2009;4(5):5947.

Hinton GE. A practical guide to training restricted boltzmann machines. In: Neural networks: Tricks of the trade. Springer; 2012. p. 599–619.

Hinton GE, Salakhutdinov RR. Reducing the dimensionality of data with neural networks. science 2006;313(5786):504–7.

Hoffman MD, Blei DM, Wang C, Paisley J. Stochastic variational inference. Journal of Machine Learning Research 2013;14:1303–47.

Hopfield JJ. Artificial neural networks. IEEE Circuits and Devices Magazine 1988;4(5):3–10.

Hsu WN, Zhang Y, Glass J. Learning latent representations for speech generation and transformation. arXiv preprint arXiv:170404222 2017;.

Jensen FV, Nielsen TD. Bayesian Networks and Decision Graphs. Berlin, Germany: Springer-Verlag, 2007.

Jiang Z, Zheng Y, Tan H, Tang B, Zhou H. Variational deep embedding: An unsupervised and generative approach to clustering. arXiv preprint arXiv:161105148 2016;.

Johnson M, Duvenaud DK, Wiltschko A, Adams RP, Datta SR. Composing graphical models with neural networks for structured representations and fast inference. In: Advances in neural information processing systems. 2016. p. 2946–54.

Jolliffe I. Principal component analysis. In: International encyclopedia of statistical science. Springer; 2011. p. 1094–6.

Jordan MI, Ghahramani Z, Jaakkola TS, Saul LK. An introduction to variational methods for graphical models. *Machine learning* 1999;37(2):183–233.

Kingma DP, Mohamed S, Jimenez Rezende D, Welling M. Semi-supervised learning with deep generative models. In: Ghahramani Z, Welling M, Cortes C, Lawrence ND, Weinberger KQ, editors. Advances in Neural Information Processing Systems 27. Curran Associates, Inc.; 2014. p. 3581–9. URL: <http://papers.nips.cc/paper/5352-semi-supervised-learning-with-deep-generative-models.pdf>.

Kingma DP, Welling M. Auto-encoding variational Bayes. arXiv preprint arXiv:13126114 2013;.

Kipf TN, Welling M. Variational graph auto-encoders. arXiv preprint arXiv:161107308 2016;.

Koller D, Friedman N. Probabilistic graphical models: principles and techniques. MIT press, 2009.

Kucukelbir A, Tran D, Ranganath R, Gelman A, Blei DM. Automatic differentiation variational inference. *The Journal of Machine Learning Research* 2017;18(1):430–74.

Kulkarni TD, Whitney WF, Kohli P, Tenenbaum J. Deep convolutional inverse graphics network. In: Advances in neural information processing systems. 2015. p. 2539–47.

Lauritzen SL. Propagation of probabilities, means, and variances in mixed graphical association models. *Journal of the American Statistical Association* 1992;87(420):1098–108.

LeCun Y, Bottou L, Bengio Y, Haffner P. Gradient-based learning applied to document recognition. *Proceedings of the IEEE* 1998;86(11):2278–324.

Li M, Zhang T, Chen Y, Smola AJ. Efficient mini-batch training for stochastic optimization. In: *Proceedings of the 20th ACM SIGKDD international conference on Knowledge discovery and data mining*. ACM; 2014. p. 661–70.

Linderman SW, Miller AC, Adams RP, Blei DM, Paninski L, Johnson MJ. Recurrent switching linear dynamical systems. *arXiv preprint arXiv:161008466* 2016;.

Louizos C, Shalit U, Mooij JM, Sontag D, Zemel R, Welling M. Causal effect inference with deep latent-variable models. In: *Advances in Neural Information Processing Systems*. 2017. p. 6446–56.

Maddison CJ, Mnih A, Teh YW. The concrete distribution: A continuous relaxation of discrete random variables. *CoRR* 2016;abs/1611.00712. URL: <http://arxiv.org/abs/1611.00712>. arXiv:1611.00712.

Masegosa A, Nielsen TD, Langseth H, Ramos-Lopez D, Salmerón A, Madsen AL. Bayesian models of data streams with hierarchical power priors. *arXiv preprint arXiv:170702293* 2017a;.

Masegosa AR, Martinez AM, Langseth H, Nielsen TD, Salmerón A, Ramos-López D, Madsen AL. Scaling up Bayesian variational inference using distributed computing clusters. *International Journal of Approximate Reasoning* 2017b;.

Minka TP. Expectation propagation for approximate Bayesian inference. In: *Proceedings of the Seventeenth conference on Uncertainty in artificial intelligence*. Morgan Kaufmann Publishers Inc.; 2001. p. 362–9.

Mnih A, Gregor K. Neural variational inference and learning in belief networks. *arXiv preprint arXiv:14020030* 2014;.

Mnih A, Rezende DJ. Variational inference for Monte Carlo objectives. arXiv preprint arXiv:160206725 2016;.

Murphy KP. Machine learning: a probabilistic perspective. MIT press, 2012.

Murphy KP, Weiss Y, Jordan MI. Loopy belief propagation for approximate inference: An empirical study. In: Proceedings of the Fifteenth conference on Uncertainty in artificial intelligence. Morgan Kaufmann Publishers Inc.; 1999. p. 467–75.

Paszke A, Gross S, Chintala S, Chanan G, Yang E, DeVito Z, Lin Z, Desmaison A, Antiga L, Lerer A. Automatic differentiation in PyTorch. 2017. NIPS AutoDiff Workshop.

Pearl J. Probabilistic Reasoning in Intelligent Systems: Networks of Plausible Inference. San Mateo, CA.: Morgan Kaufmann Publishers, 1988.

Pless R, Souvenir R. A survey of manifold learning for images. IPSJ Transactions on Computer Vision and Applications 2009;1:83–94.

Plummer M. JAGS: A program for analysis of Bayesian graphical models using Gibbs sampling. In: Proceedings of the 3rd international workshop on distributed statistical computing. Vienna, Austria; volume 124; 2003. .

Pritchard JK, Stephens M, Donnelly P. Inference of population structure using multi-locus genotype data. Genetics 2000;155(2):945–59.

Pu Y, Gan Z, Henao R, Yuan X, Li C, Stevens A, Carin L. Variational autoencoder for deep learning of images, labels and captions. In: Advances in neural information processing systems. 2016. p. 2352–60.

Ranganath R, Gerrish S, Blei D. Black box variational inference. In: Artificial Intelligence and Statistics. 2014. p. 814–22.

Rezende DJ, Mohamed S, Wierstra D. Stochastic backpropagation and approximate inference in deep generative models. arXiv preprint arXiv:14014082 2014;.

Robbins H, Monro S. A stochastic approximation method. *The annals of mathematical statistics* 1951;:400–7.

Ruiz FR, AUEB MTR, Blei D. The generalized reparameterization gradient. In: Advances in Neural Information Processing Systems. 2016. p. 460–8.

Russell SJ, Norvig P. Artificial intelligence: A modern approach. Pearson, 2016.

Salakhutdinov R. Learning deep generative models. *Annual Review of Statistics and Its Application* 2015;2:361–85.

Salmerón A, Cano A, Moral S. Importance sampling in Bayesian networks using probability trees. *Computational Statistics & Data Analysis* 2000;34(4):387–413.

Salvatier J, Wiecki TV, Fonnesbeck C. Probabilistic programming in Python using PyMC3. *PeerJ Computer Science* 2016;2:e55.

Schölkopf B, Smola A, Müller KR. Nonlinear component analysis as a kernel eigenvalue problem. *Neural computation* 1998;10(5):1299–319.

Schulman J, Heess N, Weber T, Abbeel P. Gradient estimation using stochastic computation graphs. In: Advances in Neural Information Processing Systems. 2015. p. 3528–36.

Semeniuta S, Severyn A, Barth E. A hybrid convolutional variational autoencoder for text generation. *arXiv preprint arXiv:170202390* 2017;.

Sohn K, Lee H, Yan X. Learning structured output representation using deep conditional generative models. In: Advances in Neural Information Processing Systems. 2015. p. 3483–91.

Tipping ME, Bishop CM. Probabilistic principal component analysis. *Journal of the Royal Statistical Society: Series B (Statistical Methodology)* 1999;61(3):611–22.

Titsias M, Lázaro-Gredilla M. Doubly stochastic variational Bayes for non-conjugate inference. In: International Conference on Machine Learning. 2014. p. 1971–9.

Tran D, Hoffman MW, Moore D, Suter C, Vasudevan S, Radul A. Simple, distributed, and accelerated probabilistic programming. In: Advances in Neural Information Processing Systems. 2018. p. 7608–19.

Tran D, Kucukelbir A, Dieng AB, Rudolph M, Liang D, Blei DM. Edward: A library for probabilistic modeling, inference, and criticism. arXiv preprint arXiv:161009787 2016;.

Tucker G, Mnih A, Maddison CJ, Lawson J, Sohl-Dickstein J. Rebar: Low-variance, unbiased gradient estimates for discrete latent variable models. In: Advances in Neural Information Processing Systems. 2017. p. 2627–36.

Wainwright MJ, Jordan MI. Graphical models, exponential families, and variational inference. Foundations and Trends® in Machine Learning 2008;1(1–2):1–305.

Williams RJ. Simple statistical gradient-following algorithms for connectionist reinforcement learning. Machine learning 1992;8(3–4):229–56.

Wingate D, Weber T. Automated variational inference in probabilistic programming. arXiv preprint arXiv:13011299 2013;.

Winn JM, Bishop CM. Variational message passing. Journal of Machine Learning Research 2005;6:661–94.

Xie J, Girshick R, Farhadi A. Unsupervised deep embedding for clustering analysis. In: International conference on machine learning. 2016. p. 478–87.

Zhang C, Butepage J, Kjellstrom H, Mandt S. Advances in variational inference. IEEE transactions on pattern analysis and machine intelligence 2018;.

Zhou M, Cong Y, Chen B. The poisson gamma belief network. In: Advances in Neural Information Processing Systems. 2015. p. 3043–51.